Time-Resolved Fluorescence Quenching in Micellar Assemblies

Marcelo H. Gehlen† and Frans C. De Schryver*

Department of Chemistry, Katholieke Universiteit Leuven, Celestijnenlaan 200 F, B 3001 Heverlee, Belgium

Received June 30, 1992 (Revised Manuscript Received October 29, 1992)

Contents

I. Introduction

The self-assembly of amphiphilic species in water giving rise to the formation of "molecular clusters" called micelles is one of the central research topics in colloid science. The use of micelles as a convenient way to concentrate reactants in photoprocesses was first recognized by Förster and Selinger[1] in their study of energy transfer. A substantial body of research has been dedicated to photophysics and photochemistry in micellar solution.[2-11] The study of photophysical properties, such as fluorescence excitation and emission spectra and their shifts, the relative intensity of vibronic bands, anisotropy, quantum yields, and excited-state lifetimes, of probes has provided significant information on the micellar structure at the molecular level.[2-5] Micelle formation, determination of the critical micellar concentration, cmc, and micellar characteristics, such as polarity, viscosity, and ion density can be investigated by selecting an appropriate fluorescent probe. The fluorescence quenching in micelles is, nowadays, a valuable tool to measure micellar size as well as the dynamic properties of the aggregate and of the solubilized species in the host structure.[6-10]

* To whom correspondence should be addressed.
† Permanent address: IFQSC, Universidade de São Paulo, São Carlos, 13560, SP, Brazil.

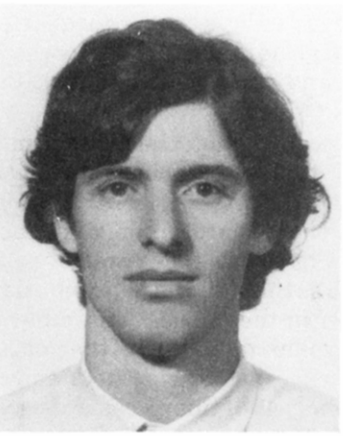

Marcelo Henrique Gehlen graduated in Chemistry at Universidade do Rio Grande Sul. He received his M.S. degree from Universidade de São Paulo in 1989, and joined the Instituto de Física e Química de São Carlos as an assistant researcher. He spent two years at Katholieke Universiteit Leuven as a doctoral fellow with Frans De Schryver. His research interests are in the area of chemical kinetics in microheterogeneous systems.

F. C. De Schryver was born in 1939 in Belgium and obtained his doctoral degree at the K.U. Leuven in 1964. He spent almost two years as a Fulbright postdoctoral Fellow with the late "Speed" C. S. Marvel at the University of Arizona and was introduced to the field of photophysics by a short stay at the laboratories of the late Prof. Forster and of Prof. Weller. He became full professor at the University of Leuven in 1975 were he has developed a group interested in fundamental and applied aspects of photochemistry and photophysics. He has been a visiting professor at a number of universities and is a part time staff member at the Université de Louvain. Since 1989 he has been a member of the Royal Academy of Belgium. He has served the photochemistry community in numerous functions and was chairman of EPA and of the IUPAC Photochemistry Commission. In 1992 he was chairman of the IUPAC Symposium on Photochemistry.

The proper organization of the reactants at the molecular level usually leads to a higher efficiency of several types of photoprocesses such as energy transfer, fast photoredox reactions, and photoionization when

0009-2665/93/0793-0199$12.00/0 © 1993 American Chemical Society

carried out in the micellar phase.[11] The presence of a charged interface in the case of ionic micelles allows, in some circumstances, a more efficient radical separation, e.g., via ejection of formed radicals with the same charge sign as that of the micellar surface. In such conditions, where the back reaction is reduced, the photoproducts can be used in a sequential step with a much higher overall yield. Through exploration of the best conditions for a given photoprocess, functionalized micellar systems have been designed to form the required micellar architecture. Photophysics and photochemistry in a microheterogeneous system therefore not only have "enlightened" micellar structure and dynamics but also are active fields in which the coupling of structure and reactivity has allowed an optimizing feedback.

Photophysics and photochemistry in micellar solution and related topics have been reviewed in several places.[2-11] In the present contribution attention is centered on the description of dynamic fluorescence quenching in micelles. The controlling factors of this process, such as the statistical distribution of the probe and quencher in the micellar ensemble and the intra- and intermicellar mobility of the reactants, are described, and experimental methods and new strategies in the data analysis of fluorescence decays obtained by the time-correlated single-photon counting are discussed. This requires a brief description of the structural and dynamic properties of micellar assemblies such as those formed by surfactants, polymer surfactant clusters, and block polymers, which are some of the target systems currently investigated by fluorescence quenching methods.

I.1. Micellar Structure

Surfactants are amphiphilic molecules composed of a polar group bound to a hydrophobic moiety, usually a long carbon chain, and are classified as anionic, cationic, or nonionic depending on the nature of the polar or head group.[12] The most simple picture of the micellar structure formed by ionic surfactants is the Hartley model.[13] In this model micelles are considered as globular structures having a hydrocarbon core surrounded by a highly hydrophilic region formed by the surfactant head groups, counterions, and water molecules. Several aspects of this self-assembled structure such as the degree of ion binding, the extent of the water penetration into the structure, and the statistical conformation of the surfactant chains have been subject of discussion.[14-17] Alternative models of the micelle structure have then been suggested to better explain those details. The Menger model,[15] describing micelles as more open structures containing a series of microchannels allowing deeper water penetration, the Dill–Flory model,[16] based on a description of a statistic conformational distribution of the surfactants chains in a multilayer lattice, and the surfactant-block structure as suggested by Fromherz[17] are some examples of more sophisticated models. In the formulation of the fluorescence quenching process, the micelle is described as forming, on the time scale of the experiment, a well-defined microdomain allowing the compartmentalization of the probe and quencher. In small micelles the quencher occupancy is treated as a discrete variable. The statistical distribution of the probe and quencher

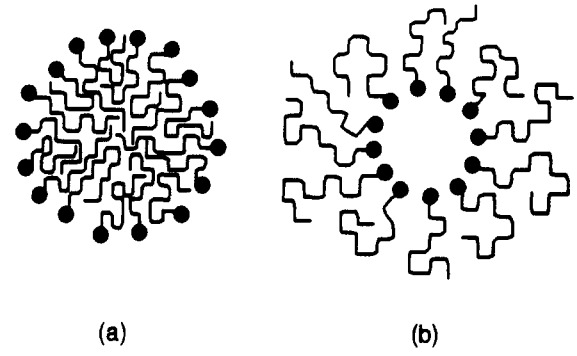

Figure 1. Micellar structures: (a) aqueous spherical micelles; (b) reverse micelle.

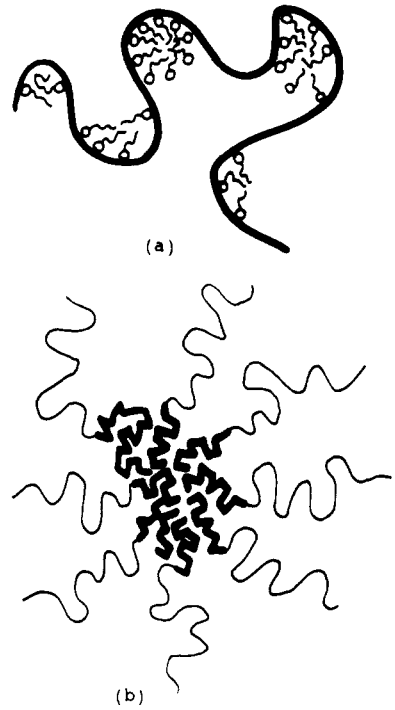

Figure 2. Micellar structures involving polymers: (a) polymer surfactant cluster; (b) self-assembly of a diblock polymer.

among the micelles is an important point in the description of the fluorescence quenching process (vide infra).

The general character of the fluorescence quenching models in aqueous micelles formed by surfactant has allowed their application in the study of micelle-like structures such as those formed in polymer–surfactant solution, block copolymers forming micelles in certain solvents, and copolymers containing a hydrophobic pendant group inducing the macromolecule to a micelle-like shape in water. A schematic representation of those systems is shown in Figure 2.

I.2. Micellar Dynamics

Micelles formed by surfactants are dynamic structures displaying a complex formation–breakdown process.[18-25] The kinetics of micellization in the aqueous phase have been discussed on the basis of the Aniansson–Wall model.[18,19] The most relevant feature of that model is the prediction of two well-separated relaxation times. Experiments indicate that the residence time of a micelle at a given aggregation number is of the

order of 0.2–10 μs, while the mean lifetime of a micelle belongs to the millisecond time scale. Since the time window usually applied in time-resolved fluorescence quenching experiments does not exceed a few microseconds micelles can be assumed to be frozen aggregates or in some cases aggregates subject to fluctuations of the monomer number and hence in micellar volume of only a few percent of the average size value. In the case of a micelle solution in the presence of additives such as short-chain alcohols, the formation–breakdown processes of the micelle can be fast enough to allow probe and quencher to be exchanged between micelles during the fluorescence decay. From measurement of these exchange rates by fluorescence quenching methods, the dynamic properties and the stability of micelles can be investigated. Not much information about relaxation processes in polymer–surfactant clusters is available. However, when the polymer chain is by adsorption wrapped around the micellar aggregate, one expects a slowing down of these processes compared to those in a micellar solution in the absence of polymer. On the other hand, if the surfactant monomers are forming several local clusters, supported along the polymer chain, relaxation process are likely to be enhanced due to the easier motion of the monomer along the chain. A possible structure of a polymer-surfactant cluster is presented in Figure 2a.

In the case of micelles formed by self-assembly of single diblock copolymer chains (Figure 2b), relaxation processes are also predicted to occur but at a time scale several orders of magnitude slower than those observed in micelles formed by surfactants.[26,27]

II. Theory of the Intramicellar Fluorescence Quenching

II.1. Diffusion-Controlled Processes in Micelles

Consider the case of a micelle containing one excited probe and one quencher. The deactivation of the probe via a quenching process can be described by

$$P^* + Q \xrightarrow{k_1} [P^*\cdots Q] \xrightarrow{k_2} P + Q \qquad (1)$$

Assuming a diffusion-controlled process (e.g., $k_2 \gg k_1$) and in absence of long-range interparticle potential, the pair distribution density $p(r,t)$ satisfies

$$\partial p/\partial t = D\nabla^2 p \qquad (2)$$

where D is the mutual diffusion coefficient of the probe and quencher and ∇^2 is the Laplacian operator. Several limiting situations for the probe–quencher distribution in the micelle, giving rise to slightly different models, have been analyzed: (a) The probe resides at the center of a spherical micelle, and the quencher moves freely in the micelle.[29,30] (b) The quencher resides at the micelle–water interface forming a homogeneous reactive surface, and the probe moves freely in the micelle.[30] (c) Both quencher and probe move in a tangential way at a fixed distance R from the center of the micelle (R being close to the micelle radius).[31,32]

In all cases the quenching process is assumed to occur at the first encounter of the probe and quencher (Smoluchowski condition). The solution of eq 2 subjected to the particular boundary conditions and the symmetries imposed on the Laplacian operator has been discussed in detail for each of these three models. Experimentally, the measurable quantity is the spatially averaged pair density, $\langle p \rangle$. In the model a, $\langle p \rangle_a$ is given by the following exponential series:

$$\langle p \rangle_a = \sum_n C_n \exp[-Dx_n^2 t/r_0^2] \qquad (3)$$

$$C_n = 6z^2/\{(1-z^3)x_n^2[(1-z) - (1+x_n^2)^{-1}]\} \qquad (4)$$

where $z = (R_q + R_p)/r_0$, $r_0 = R_m - R_q$. R_q, R_p, and R_m are the quencher, probe and micelle radius respectively, while x_n represents the positive roots of

$$x_n \cot(1-z)x_n - 1 = 0 \qquad (5)$$

Hatlee et al. evaluated the decay curves as described by eq 3 for values of the parameters D, r_0, and z as could be typically expected for micellar aggregates. They observed that for values of $D = (1–5) \times 10^{-7}$ cm^2 s^{-1} and $(R_q + R_p)/(R_m - R) = 0.2–0.4$, the first coefficient C_1 of eq 3 is practically 1. Since all coefficients C_n are positive and normalized, it indicates that eq 6 is a good approximation for $\langle p \rangle_a$:

$$\langle p \rangle_a = \exp[-Dx_1^2 t/r_0^2] \qquad (6)$$

An analytical solution has been obtained also for model b. The solution for the "survival probability" of the excited probe is expressed by a series with a similar exponential form as in model a:

$$\langle p \rangle_b = (6/\pi^2)\sum_n (1/n^2) \exp[-(n\pi)^2 Dt/r_0^2] \qquad (7)$$

In a time domain where $t > r_0^2/\pi^2 D$, the first term of the summation in eq 7 will dominate the kinetic behavior of the quenching process. For spherical micellar aggregates, the ratio $r_0^2/\pi^2 D$ is on the order of 10 ns. As a result, the quenching process will exhibit essentially first-order kinetics for times longer than 10 ns.

If fluorescence quenching occurs via diffusion of the probe and quencher on the micellar surface (case c), the spatially averaged pair density is expressed as

$$\langle p \rangle_c = \sum_i \alpha_i \exp[-s_i(s_i+1)D_s t/R^2] \qquad (8)$$

where the coefficients α_i involve the surface integral of Legendre series of order s_i. R is a distance from the micelle center forming a spherical shell, and D_s is the sum of the tangential diffusion coefficients of the probe and quencher in the shell. For values of D_s/R^2 larger than 1, the decay is always exponential (Figure 3); at smaller values, however, the decay is nonexponential. Extrapolating the exponential part of the decay to ln $\langle p(t=0) \rangle_c$ gives an intercept which is a measure for the error, assuming the absence of transient effects on the decay. Since those transient effects are small, the exponential decay is also in this case a good approximation of the time evolution of the spatially averaged pair density.

The kinetics of a diffusion-controlled quenching process in micelles has also been investigated on the

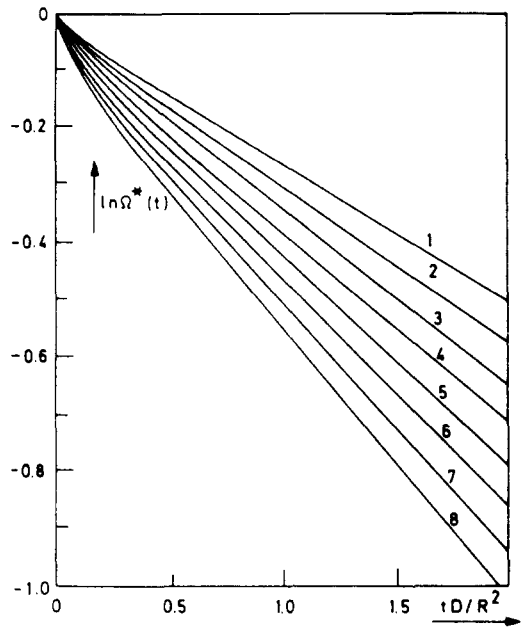

Figure 3. Plot of the ln $\langle p(t)\rangle_c$ versus reduced time for different probe–quencher encounter angles in the tangential diffusion in a spherical micelle: (1) $\theta_{pq} = 0.15$; (2) $\theta_{pq} = 0.2$; (3) $\theta_{pq} = 0.25$; (4) $\theta_{pq} = 0.3$; (5) $\theta_{pq} = 0.35$; (6) $\theta_{pq} = 0.4$; (7) $\theta_{pq} = 0.45$; (8) $\theta_{pq} = 0.5$ (from ref 31; copyright 1981), American Institute of Physics.

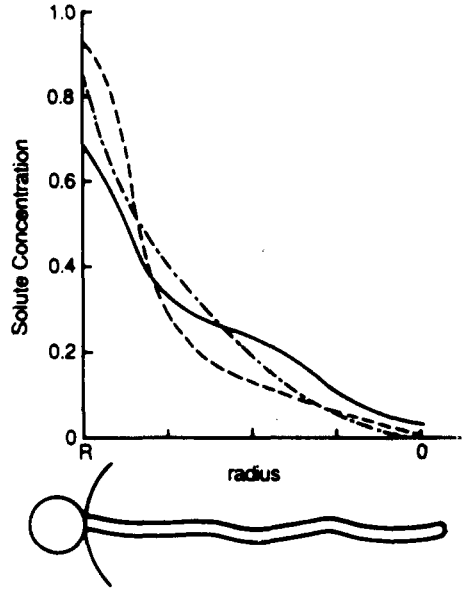

Figure 4. Solute distribution within spherical micelles. Number of lattice sites per radial layer (- · -) ideal solute with no surface activity (—), solute with surface activity (- - -) (from ref 35; copyright 1986), American Institute of Physics.

basis of random-walk simulations.[28,33,34] This approach is particularly important in situations where no analytical solution to the diffusion problem is known as well as in the test of approximate models.

The three models of fluorescence quenching briefly discussed above are necessarily approximations of the real case where preferential distribution of the solute as well as the mobility of both probe and quencher over the whole micellar volume can be present. However if one takes into account the theoretical prediction for the solute distribution within a micelle[35] and the experimental evidence obtained using environment sensitive probes,[36] one realizes that the diffusional motion of the partners near or at the micellar surface is physically more meaningful. The solute distribution within spherical micelles based on the lattice model of Dill is shown in Figure 4.

A common feature of the three models is the prediction of an exponential decay of the survival probability of the excited probe at long times. If the transient effects are small, $\langle p\rangle$ equals

$$\langle p\rangle \cong \exp[-k_q t] \tag{9}$$

where k_q is the model-related quenching rate constant. It carries information concerning the diffusion coefficient and size parameters of the probe and quencher as well as the structure factors of the micelle such as the micellar average radius.

In micellar fluorescence quenching experiments, frequently a micelle containing one excited probe can be occupied by several quenchers. Assuming that the quenchers are randomly distributed in a micelle and moving independently of each other, the probability that at a time t the fluorescent probe has not yet met any of the quenchers is then given by[29,37]

$$\bar{p}(n,t) = \prod_{i=1}^{n} \langle p_i\rangle = \langle p_1\rangle^n \tag{10}$$

and the concentration-dependent quenching rate at long times equals

$$k_{q,n} = -\partial \ln \bar{p}(n,t)/\partial t = nk_q \tag{11}$$

Equation 11 shows that the quenching probability is linearly proportional to the occupancy. This fact provides the basic argument for the stochastic description of the fluorescence quenching process.

II.2. Stochastic Description of the Quenching Process in Micelles

The solubilization of a quencher in a micellar solution gives rise to a distribution process of the quenchers over the micellar ensemble. The micelle subsets containing 0, 1, 2, ..., quenchers are characterized by a distribution function with a finite average occupancy $\bar{n}$. Due to size restrictions of the micelle, $\bar{n}$ is usually small. Time fluctuations in the number of quenchers in a micelle of the order of $\bar{n}$ will require a stochastic treatment of the quenching process. The basic model[38-48] where the quencher is considered as an immobile or mobile species and the probe is considered as an immobile species remaining in the same micelle during its excited-state lifetime is discussed. The general case where both species are considered mobile during the time window of the fluorescence quenching process is also discussed within the framework of a stochastic treatment.[49-54]

II.2.1. Mobile Quencher–Immobile Probe

It has been demonstrated that the deactivation rate of an excited probe in a micelle occupied by n quenchers is in a good approximation given by the product of the occupancy n times the fluorescence quenching rate constant k_q. For partially bound quenchers, the actual number of quenchers in a micelle containing one excited probe can be subject to an increment in this number due to the inward flux from the quenchers in the

aqueous phase or a decrement due to the exit of quenchers from the micelle. The process by which the quencher binds to or leaves the micelle is usually represented by

$$M_n + Q_a \xrightarrow{k_+[Q]_a} M_{n+1}$$

$$M_n \xrightarrow{nk_-} M_{n-1} + Q_a \quad (12)$$

where k_+ and k_- are the second-order rate constant for the entry of a quencher molecule into the micelle and the first-order rate constant for exit of a quencher molecule from a micelle, respectively. $[Q]_a$ is the equilibrium concentration of the quencher molecules in the aqueous phase. For the scheme considered above, the probability of finding a micelle with n quenchers is given by a Poisson distribution:

$$P_n = \frac{[M_n]}{[M]} = \frac{\bar{n}^n}{n!}\exp[-\bar{n}] \quad (13)$$

where $[M_n]$ and $[M]$ denote the concentration of micelles with n quenchers and the total micelle concentration, respectively, and $\bar{n}$ is the average numbers of quencher per micelle:

$$\bar{n} = k_+[Q]_a/k_- \quad (14)$$

$\bar{n}$ can be defined in terms of the known or measurable quantities of the total quencher concentration, [Q], and the micelle concentration. The former is expressed as

$$[Q] = \bar{n}[M] + [Q]_a \quad (15)$$

Elimination of $[Q]_a$ from eqs 14 and 15 leads to

$$\bar{n} = \frac{K[Q]}{1 + K[M]} \quad (16)$$

where $K = k_+/k_-$.

The total micelle concentration is usually calculated by

$$[M] = \frac{[S] - cmc}{N_{agg}} \quad (17)$$

where [S], cmc, and N_{agg} denote the surfactant concentration, the critical micellar concentration, and the average aggregation number, respectively.

For an excited probe in a micelle containing n quenchers, the natural decay of the excited probe and the intramicellar quenching process are given respectively by

$$M^*_n \xrightarrow{k_0 + nk_q} M_n \quad (18)$$

The probability of finding a micelle with one excited probe and n quencher molecules at time t, $P^*_n(t)$, is the solution of the following stochastic equation:[39]

$$dP^*_n/dt = -\{k_0 + k_+[Q]_a + (k_q + k_-)n\}P^*_n + k_+[Q]_aP^*_{n-1} + (n+1)k_-P^*_{n+1} \quad (19)$$

with the initial condition $P^*_n(0) = P_n$.

The time-dependent fluorescence signal, $f(t)$, is proportional to the total survival probability $\sum_n P^*_n$. Equation 19 can be solved by the generating function method in order to determine $f(t)$. The expression for the fluorescence decay after a δ-pulse excitation is

$$f(t) = A_1 \exp[-A_2t + A_3(\exp[-A_4t] - 1)] \quad (20)$$

where

$$A_1 = f(0) \quad (21)$$

$$A_2 = k_0 + \frac{k_qk_-\bar{n}}{k_- + k_q} \quad (22)$$

$$A_3 = \frac{\bar{n}k_q^2}{(k_q + k_-)^2} \quad (23)$$

$$A_4 = k_q + k_- \quad (24)$$

If the quencher molecules do not exchange via the water phase within the time scale of the excited state of the probe, eq 20 is reduced to

$$f(t) = A_1 \exp[-k_0t + \bar{n}(\exp[-k_qt] - 1)] \quad (25)$$

Equations 20 and 25 have been applied with success in the description of the fluorescence quenching of an immobile probe by mobile (eq 20) or immobile (eq 25) quenchers in aqueous micelles.[55-89] The average micellar aggregation number, N_{agg}, as well as the rate constants of the association and dissociation of the quencher have been determined from appropriate fitting of decays curves to these model equations. Parameters obtained from analysis of time-resolved fluorescence quenching in aqueous micelles are summarized in Tables I, IIa, and IIb.

The fluorescence quenching of pyrene derivatives such as 1-methylpyrene by alkylpyridinium chloride is in a great number of aqueous micellar systems a diffusion-controlled process.[80,87,88,134] Depending on the length of the alkyl tail with respect to the length of the micellar alkyl chain, these kind of quencher molecules can behave as an immobile or as a mobile species.[87] Usually in anionic micelles, such as those formed by sodium dodecyl sulfate (SDS), the decylpyridinium ions are already "immobile". In cationic micelles such as those formed by hexadecyltrimethylammonium chloride (CTAC), this condition is fulfilled starting from tetradecylpyridinium chloride.[87] Figure 5 shows the dependence of $1/A_2$ values on the alkyl chain length of alkylpyridinium chloride quenchers as obtained by the fluorescence quenching of 1-methylpyrene in the anionic as well as cationic micellar systems. The horizontal lines represent the values of the probe decay time in the absence of added quencher. Experimentally, the quencher is considered immobile if $1/A_2$ is independent of the quencher concentration and its value is equal to the probe decay time. These results demonstrate that the residence time of an ionic quencher in a micelle depends strongly on the balance between the electrostatic and hydrophobic contributions involved in the association process of the quencher to the micellar host structure.

When hydrophilic and ionic quenchers are used, a dependence of the exit rate constant of the quencher from the micelle on the micelle concentration has been observed.[43,59-62] To explain the quenching of pyrene by metal ions in SDS, an additional process for the exchange of the quencher involving micelle interaction

Table I. Fluorescence Quenching in Aqueous Micelles in the Absence of Intramicellar Exchange[a]

surfactant/probe/quencher systems[ref]	τ_0 (ns)	k_q (μs^{-1})	N_{agg}
SDS (0.07 M)/Ru(bipy)$_3^{2+}$/9-MeA[65]			
NaCl (M)			
0	480	20.40	63
0.30		12.30	104
0.45		8.67	134
0.60		3.76	260
0.75		2.40	373
SDS (0.1 M)/1-MePy/C_{10}PyCl[88]			
n-butanol (M)			
0	200	35.5	68
0.327		64.6	48
0.545		65.2	40
0.654		82.3	28
1.090		98.6	19
n-decanol (M)			
0.01		23.5	92
0.02		22.0	104
0.03		19.0	124
SDS (0.05 M)/Ru(phen)$_3^{2+}$/alkylviologen[74]			
methyl	6250	0.84	
ethyl		0.71	
propyl		0.54	
butyl		0.52	
hexyl		0.39	
	2270	1.66	
SDS (0.05 M)/Ru(dpphen)$_3^{2+}$/methyl			
ethyl		0.96	
propyl		0.67	
butyl		0.42	
hexyl		0.23	
SDS (0.2 M)/pyrene/excimer form[70]			
n-pentanol (M)			
0	360	17.5	66
0.6	408	18.3	45
0.8	406	8.3	95
1.0	410	6.6	130
SDS (0.05 M)/C_4PyN^+/C_{12}PyCl[123b]	204	37.0	64
SDOC (4%)/pyrene/excimer form[81]	410	14.4	11
TTOES (0.01 M)/Ru(bipy)$_3^{2+}$/MPTH[40]	667	3.0	95
CTAC (0.031 M)/1-MePy/C_{14}PyCl[80]			
NaCl (M)			
0	187	14.0	89
0.050		11.0	107
0.083		9.0	127
0.104		9.0	136
0.155		8.5	176
CTAC, M/pyrene/C_{16}PyCl[83]			
0.120	332	10.2	117
0.205	330	10.0	119
0.460	328	8.8	135
0.730	332	8.4	145
CRAC, M/pyrene/excimer form[83]			
0.016	329	8.40	91
0.031	330	7.90	99
0.064	340	6.80	106
0.123	345	6.10	118
0.254	341	5.70	124
0.300	327	5.70	128
0.465	334	5.20	134
0.740	332	5.00	143
0.991	314	4.40	154
1.204	332	3.60	187
CTAC (0.05 M)/ZnP/$C_{11}H_{23}$-duroquinone[64]	0.20 ms	5.0	
CTAOAc (0.03 M)/pyrene/DBA[89]	178	4.44	70
TTAC (0.05 M)/1-MePy/MDA[79]		33.4	67
DTAC (0.031 M)/1-MePy/C_{14}PyCl[80]			
NaCl (M)			
0	187	50.0	47
0.020		47.3	48
0.072		41.7	53
0.155		36.0	56
0.310		31.7	63
0.520		31.7	65
DTAC (0.1 M)/1-MePy/C_{14}PyCl[88]			
n-butanol (M)			
0	187	46.7	48
0.219		51.1	40
0.328		60.2	37
0.545		68.8	32
0.654		75.9	28
0.854		100.1	24
n-decanol (M)			
0.005		45.0	52
0.010		35.3	53
0.015		31.2	60
0.020		28.9	64
0.030		24.3	70
DTAC (0.1 M)/1-MePy/C_{14}PyCl[85]	187	47.0	47

[a] Surfactants: SDS = sodium dodecyl sulfate; SDOC = sodium deoxycholate; TTOS = sodium tetradecyltrioxyethylene sulfate; CTAC = hexadecyltrimethylammonium chloride; TTAC = tetradecyltrimethylammonium chloride; DTAC = dodecyltrimethylammonium chloride; CTAOAc = hexadecyltrimethylammonium acetate. Probes: Ru(L)$_3^{2+}$ = ruthenium complex, bipy = bipyridine, phen = phenanthroline, dpphen = 4,7-diphenylphenanthroline; 1-MePy = 1-methylpyrene; C_4PyN^+ = 1-pyrenebutyltrimethylammonium bromide; ZnP = Zinc porphyrin. Quenchers: 9-MeA = 9-methylanthracene; C_nPyCl = *N*-alkylpyridinium chloride; MPTH = *N*-methylphenothiazine; DBA = dibutylaniline; MDA = *N*-methyl-*N*-decylaniline.

was suggested[43,59]

$$M^*_n + M_j \xrightarrow{nk_e[M_j]} M^*_{n+1} + M_{j-1} \quad (26)$$

The intermicellar exchange of quenchers as described by eq 26 is called the hopping process. This process was first introduced in micellar electron-transfer kinetics.[103] The increase of the exit rate constant of the quencher from a micelle is then attributed to the effect of "close encounters" of the micelles, during which the quencher migrates from micelle to micelle. The rate constant of this process is assumed to remain constant upon addition of surfactant, and the whole change in the quencher intermicellar mobility is then attributed to an increase of the micelle concentration. The fluorescence decay in the presence of this additional exchange process of the quencher is still represented by an equation similar to eq 20, but the A_i parameters are redefined by substitution of k_- by $k_- + k_e[M]$ in eqs 22–24.

The migration of a quencher with a charge opposite to that of the micellar surface is predicted to be a function of the micelle concentration.[104-106] An increase in the micelle concentration leads to a decrease of the electrostatic potential at the micelle surface, which facilitates the escape of the counterions located in the Stern layer. The escape rate constant of cations from SDS micelles was calculated by Almgren et al. using the mean first passage time approach based on the cell model for the micellar solution.[105] They showed that the values for this rate constant are strongly dependent on the micelle concentration. Figure 6 shows the calculated and experimental values of the escape rate constant k_- for Cu^{2+} at different total SDS concentration. A similar conclusion was reached by Zana et al. in the study of intermicellar mobility of I^- as a function of the CTAC concentration.[83] Figure 7 represents a plot of the experimental determined exit rate constant of I^- as a function of CTAC micellar concentration. On

Table II

(a) Micellar Entry (k_+), Exit (k_-), and Quenching (k_q) Rate Constants for Neutral Quenchers[a]

micelle/probe/quencher[ref]	k_q (μs^{-1})	k_- (μs^{-1})	k_+ ($M^{-1}\ \mu s^{-1}$) $\times 10^{-3}$
SDS/pyrene/CH_2I_2[38]	75.0	9.5	25
SDS/pyrene/mDCB[69]	27.0	7.6	11.5
SDS/DEII/pCNT[69]	75.0	6.1	
SDS/pyrene/alkyliodate[68]			
ethyl	2.9	8.3	9.7
butyl	4.8	1.4	8.8
hexyl	5.4	0.75	7.8
octyl	5.9	0.40	6.6
SDS (M)/1-MePy/mDCB[76]			
0.07	36.0	7.4	
0.28	34.0	10.0	
0.49	31.0	8.5	
0.73	21.0	8.0	
NaCl (M)			
0	35.0	5.0	10.5
0.10	29.0	4.4	7.4
0.30	26.0	6.0	8.6
0.45	17.0	6.0	11.0
0.60	12.8	7.0	14.0
CTAC/ZnP/duroquinone[64]	5.0	0.6	50.0
CRAC/1-MePy/mDCB[80]	16.0	8.0	14.4

(b) Micellar Entry (k_+), Exit (k_- and k_e), and Quenching Rate Constants for Ionic Quenchers

micelle/probe/quencher[ref]	k_q (μs^{-1})	k_+ ($M^{-1}\ \mu s^{-1}$) $\times 10^{-3}$	k_- (μs^{-1})	k_e ($M^{-1}\ \mu s^{-1}$) $\times 10^{-3}$
SDS/1-MePy/Cu^{2+} [59]	27.0	1.2	0.12	0.6
SDS/pyrene/Eu^{3+} [59]	16.0	<1	<0.1	<0.1
SDS/pyrene/Cr^{3+}	9.8	<1	<0.1	<0.1
SDS/pyrene/Ni^{2+}	8.9	1.0	0.1	0.5
SDS/pyrene/Co^{2+}	5.4	1.0	0.1	0.7
SDS/pyrene/Pb^{2+}	9.1	7.0	0.3	0.3
SDS/pyrene/Tl^+	19.0	29.0	7.6	5.5
SDS/pyrene/Ag^+	16.0	<16.0	8.0	8.0
SDS/pyrene/Cs^+	0.3	20.0	2.0	6.0
SDS/pyrene/Cu^{2+} [61]	11.0	2.9	0.48	3.3
SDS/pyrene/Cu^{2+} [75]	25.0	1.2	0.12	0.6
DTAC/pyrene/I^- [62]	5.3	50.0	2.4	0.94
TTAC/1-MePy/I^- [79]	10.4	0.6		
CTAC (M)/1-MePy/I^- [79]				
0.011	8.71	0.54		
0.021	9.73	0.83		
0.033	9.13	0.88		
0.040	7.65	0.98		

[a] mDCB = *m*-dicyanobenzene; pCNT = *p*-cyanotoluene; DEII = diethylindoloindole.

the basis of these results, it may be possible to describe the exit rate constant by a power series expansion of the micellar concentration:

$$k_{exq} = a_1 + a_2[M] + a_3[M]^2 + \ldots \quad (27)$$

Experimental values of the exit rate constant at different micelle concentration could be then used to determine the coefficients a_i of this series. However, if a linear relation of k_{exq} with [M] is observed, it cannot be taken as a proof of hopping process. Also the changes in k_{exq} at higher micelle concentration will certainly be affected by the micellar polydispersity and by changes in the micellar structure. The influence of surfactant concentration and of organic and inorganic additives on the aggregation behavior of ionic surfactants in aqueous medium has been extensively studied on the basis of the above model and has recently been reviewed.[132]

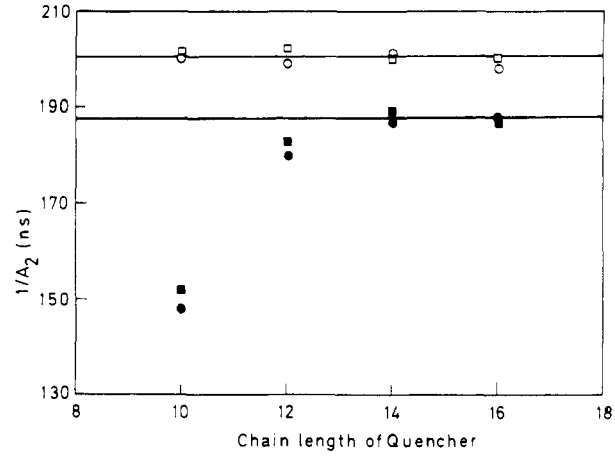

Figure 5. Dependence of $1/A_2$ values of 1-methylpyrene on the alkyl chain length of alkylpyridinium chloride quenchers ([Q] = 1.6×10^{-3} M) in 0.1 M micellar solution of SDS (○), STS (□), DTAC (●), and TTAC (■). Horizontal lines represent the values of $1/k_0$ (from ref 87; copyright 1989, American Chemical Society).

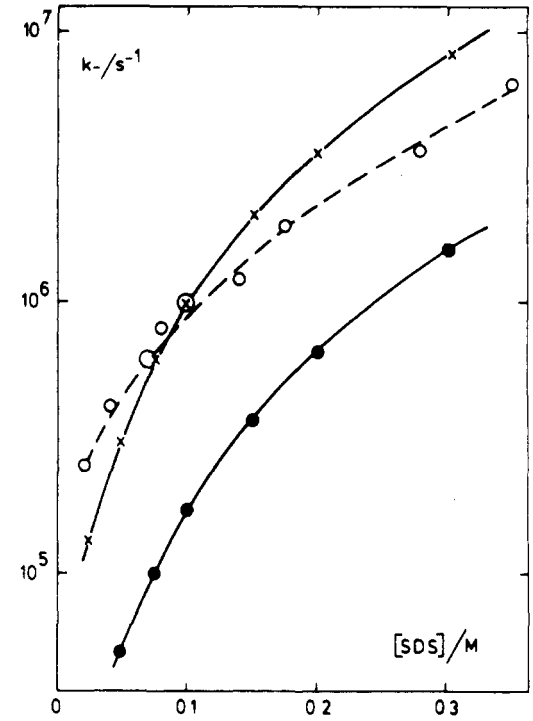

Figure 6. Escape rate constant of Cu^{2+} from SDS micelles as a function of the surfactant concentration (○). Calculated values considering the radius of closest approach of the Cu^{2+} ions to the micelle as equal to the radius of closest approach of the Na^+ (●), considering it as 1.5 Å larger than that of Na^+, experimental values (×) (from ref 105 with permission).

The hopping mechanism is more likely to occur in nonionic and reverse micellar systems where the strong electrostatic repulsion between the aggregates, present in ionic aqueous micelles, is practically absent.[107] Typically hard-sphere and short-range attractive potentials are used to describe the micelle interaction in reverse micelles.[108] The molecular transport and size characterization in reverse micelles and microemulsions has been investigated with fluorescence quenching methods.[109-122] Examples of systems investigated by this method are shown in Table III.

The physical models underlying eqs 20 and 25 have been used also to interpret fluorescence quenching in

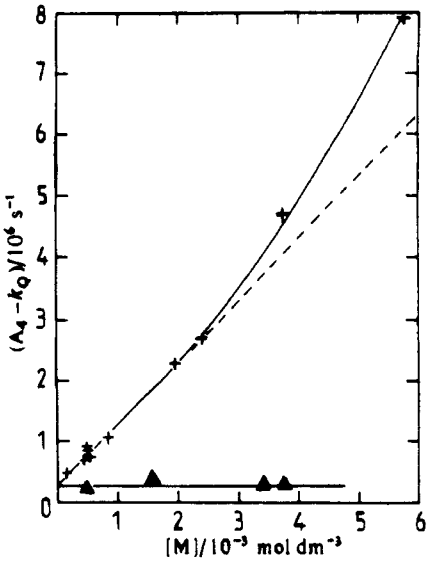

Figure 7. Variation of the intermicellar exchange rate constant, k_{exq}, with micellar concentration: (+), I^-; (▲) $C_{12}PyCl$. Dotted lines shows the predictions of the "hopping" mechanism (from ref 83; copyright 1986, Royal Society of Chemistry).

polymers forming micelles and polymer–surfactant aggregates. Those systems are likely to form microdomains in which the compartmentalization of probe and quencher results in similar quenching kinetics as that in aqueous micelles.[123-131] Some of the systems investigated are listed in Table IV. In some situations, however, the decay process of a probe in absence of added quencher may be already nonexponential due to structural disorder of the system or partition of the probe between different kinds of microdomains giving slightly different decay times. In such a case, the models described here are inadequate.

All parameters of the fluorescence quenching models in micelles may be determined by the analysis of time-resolved data. However, quite often, measurement of the quenching process using continuous excitation is used to determine the aggregation number and in some cases the binding constant of the quencher to the micelle.[90-102] To evaluate the variation of the relative fluorescence intensity as a function of the quencher concentration, the total fluorescence intensity is calculated by

$$I = k_f \int_0^\infty f(t)\, dt \qquad (28)$$

where k_f is the radiative decay rate constant. Assuming that $f(t)$ is expressed by eq 20, the ratio of the total fluorescence intensity in the presence and absence of added quencher is given by

$$\frac{I}{I_0} = \frac{k_0 \exp[-A_3]}{A_4} \int_0^1 z^{(A_2/A_4)-1} \exp[A_3 z]\, dz \qquad (29)$$

From expansion of the exponential in the integral, eq 29 can be rewritten as a series:

$$\frac{I}{I_0} = k_0 \exp[-A_3] \sum_{m=0}^{\infty} \frac{A_3{}^m}{m!(A_2 + mA_4)} \qquad (30)$$

A practical method to estimate the aggregation number was introduced by Turro and Yekta.[94] The method is

Table III. Fluorescence Quenching Data in Reverse Micelles and Microemulsions

probe/quencher	W	τ_0 (ns)	k_q (μs^{-1})	k_e ($M^{-1}\ \mu s^{-1}$) × 10^{-3}	N_{agg}
Potassium Oleate/Hexadecane/Hexanol/Water[110a]					
$Ru(bipy)_3^{2+}/Fe(CN)_6^{3-}$	16	500	2.50	0.22	
	31	571	0.45	0.28	
	53	667	0.07	0.11	
Potassium Oleate/Dodecane/Pentanol/Water[110a]					
$Ru(bipy)_3^{2+}/Fe(CN)_6^{3-}$	8.5	667	2.60	0.11	
	13	658	1.50	0.095	
	21	649	0.60	0.11	
CTAC/Dodecane/Hexanol/Water[110b]					
$Ru(bipy)_3^{2+}$/methylviologen	20.3	571	20.0		225
	40.6	588	7.0		548
	60.9	581	1.5		1250
Dodecylammonium Propionate/Cyclohexane/Water[112]					
2-(1-naphtyl)acetic acid/I^-	1.38	41.6	60	0.80	28
	2.75	42.5	40	1.30	40
	4.13	43.4	30		67
AOT/*n*-Heptane/Water[113]					
acridine/Co^{2+}	6	<32	38.0		53
	9				93
	11		21.3		100
	16		9.8		169
	18		9.4		207
	21		6.3		240
acridine/Br^-	6		80		53
	9		56		93
	11		38		100
	16		17		169
	18		12		207
	21		7.7		240
AOT/*n*-Hexane/Water[115]					
PTSA/Cu^{2+}	4	9.5	120		52
	11	10.5	70	7.0	77
	15	10.9		13.0	
	20	10.9		19.0	
PTSA/I^-	4	9.5	static		52
	7	10.2	520		73
	11	10.5	260	5.8	132
	15	10.9	100	10.2	191
	20	10.9	50	21.0	283
PSTA/SCN^-	4	9.5	300		52
	7	10.2	390		87
	11	10.5	170	6.0	117
	15	10.9	200	44.0	160
	20	10.9	200	65.0	64
CTAB/Cetyl Bromide/(Chloroform/Isooctane)/Water[119c]					
$Ru(bipy)_3^{2+}$/methylviologen	5			0.43	65
	10			0.24	180
	15			0.19	370
	20			0.30	640
	25			0.25	980
AOT/Alkane/Water[118]					
$Ru(bipy)_3^{2+}/Fe(CN)_6^{3-}$	26.3				
n-hexane				<0.07	402
n-heptane				<0.07	405
n-octane				0.1	475
n-decane				3.7	590
n-dodecane				10.0	
Benzyldimethyl-*N*-alkylammonium Chloride/Chlorobenzene/Water[119b]					
$Ru(bipy)_3^{2+}$/methylviologen					
dodecyl	10			2.3	330
tetradecyl	10			0.7	150
hexadecyl	10			0.3	70
octadecyl	10				
dodecyl	20			5.2	960
tetradecyl	20			1.0	450
hexadecyl	20			0.2	330
octadecyl	20			0.1	293

Table IV. Studies of Fluorescence Quenching of Solubilized Probes and Quenchers in Polymers and Polymers/Surfactants Systems Forming Micellar Microdomains[a]

polymer/probe/quencher	ref
PMA (pH = 5)/$Ru(bipy)_3^{2+}$/Cu^{2+}, Cr^{3+}	123c
PMA + C_{10}TAB (pH = 8)/pyrene/C_{12}PyCl	123d
PA-18K2/C_4PyN^+/C_{12}PyCl	123b
PA-6E/$Ru(bipy)_3^{2+}$/9-MeA	128
PA-1E + SDS/pyrene/excimer form	127
sodium polyacrilate + SDS/pyrene/excimer form	127
PPO + SDS/pyrene/excimer form	127
PEO + SDS/pyrene/excimer form	126, 127
PEO + SDS/pyrene/dimethylbenzophenone	129a
PEO + SDS/$Ru(bipy)_3^{2+}$/9-MeA	125
PEO–PPO–PEO triblock copolymer/pyrene/DPA	129b
PVP + SDS/$Ru(bipy)_3^{2+}$/9-MeA	125
HPC + SDS/pyrene/benzophenone	124
HPC + CTAC/pyrene/benzophenone	124a
polysaccharide hyaluronan + C_nTAB, n = 10, 12/dimethylbenzophenone	129c
starburst dentrimers + SDS/$Ru(bipy)_3^{2+}$/methylviologen	130
PPO + CTAC/1-MePy/C_{16}PyCl	131
PVOH-Ac + CTAC/1-MePy/C_{16}PyCl	131

[a] PMA = poly(acrilic acid); PEO = poly(ethylene oxide); PPO = poly(propylene oxide); PVP = poly(vinylpyrrolidone); HPC = hydroxypropylcellulose; PVOH-Ac = poly(vinyl alcohol acetate); PA-18K_2 = maleic anhydride-1-octadecene copolymer; PA-6E = maleic anhydride–hexyl vinyl ether copolymer; PA-1E = maleic anhydride–methyl vinyl ether copolymer; C_nTAB = N-alkyltrimethylammonium bromide.

based on the assumption of static intramicellar quenching. Also the probe-quencher pair must be completely bound to the micellar pseudophase. In such a situation, the fluorescence intensity will have contributions only from the subset of micelles containing the probe but being free of quencher. The relative fluorescence intensity is then

$$\frac{I}{I_0} = \exp[-\bar{n}] \tag{31}$$

From a combination of eq 31 with eqs 14–17, N_{agg} can be estimated. Later on, it was demonstrated that the apparently static quenching could result from a particular case where the excited-state lifetime of the probe is much larger than the inverse of the first-order intramicellar quenching rate constant.[66,68] When this situation occurs, eq 31 is recovered from eq 30.

A simple method to determine the binding constant, K, of a neutral quencher to the micellar phase was suggested by Encinas and Lissi:[97]

$$K = [Q]_m/[Q]_a[M] \tag{32}$$

Equation 32 can be rewritten in terms of the average number of quencher per micelle, $\bar{n}$:

$$[Q] = (\bar{n}/K) + \bar{n}[M] \tag{33}$$

K can be determined by plotting the total quencher concentration [Q] required to attain a fixed I_0/I value as a function of the micelle concentration. To apply the method, the average aggregation number of the micelles should be known a priori. For micellar systems with a strong dependence of the N_{agg} on the surfactant concentration, the method fails since an assumption inherent to the model, that fluorescence quenching is "solely" controlled by $\bar{n}$, is not longer valid. The change in micellar size does lead to changes in the first order intramicellar rate constant.

II.2.2. Mobile Quencher and Probe

The fluorescence quenching method has in principal a broad applicability in the study of micellar solutions. By this technique, micelles could be investigated in different conditions going from low to high surfactant concentration or even in the presence of electrolytes, alcohols, or other additives capable of changing the micelle size or to affect the partition coefficient of solubilized species. In fact this is an advantage of the fluorescence quenching method over other traditional methods.

In the above discussed model, the probe is considered as an immobile species remaining during its excited-state lifetime in the same micelle. Although this condition may be justified for probes with high hydrophobic character and at moderate micelle concentrations, it could however be an improper assumption either in the case of a system containing an amphiphilic probe which could migrate to a neighboring micelle through the bulk phase during micelle interaction or in the case of a solution of ionic micelles at high surfactant concentration where intermicellar exchange of both probe and quencher may occur via a coalescence–fragmentation process.[84,87] In the case of reverse micelles and of microemulsions, the postulated mechanism for exchange of solubilized species in the water droplets is the so-called fusion–fission process.[107,111,116]

In the probe migration model the exchange occurs as a result of the micelle interaction and its rate constant may be understood as the inverse of the mean first passage time of the probe between the two micellar surfaces.[134] In the other two models, the exchange occurs in a quite different way. The coalescence–fragmentation process as well as the fusion–fission process postulates the existence of transient or temporary structures. The former process considers the exchange of reactants as a result of the micelle breakdown giving rise to submicelles which can transport the reactants. In a subsequent collision with another micelle, the submicelles transfer their contents. In the fusion–fission process, micelles collide and fuse to a large aggregate, which again divides into two separate micelles. After this "sticky collision", the probes and quenchers are randomly distributed between the two micelles. If the temporary aggregates, the submicelles or the large micelle, are short-lived, the size distribution may remain narrow.

However, the postulation of the presence of temporary aggregates of a size different of the average of the micellar ensemble may have an effect on the quenching process. It was demonstrated that the intramicellar diffusion-controlled rate constant of the quenching process, k_q, is a function of the micellar size.[28-33] During the elapsed time in which the excited probe and quencher are confined to a temporary aggregate, the quenching probability will change due to changes in the reactant density and k_q as well. Since those processes for exchange of reactants are based on a diffusion process which takes place probably in the same time scale as that of quenching process, k_q is not well represented by its average value as would be in the case when nontemporary aggregates are present and the

micelle polydispersity is small. In the fusion–fission mechanism, random mixing of reactants requires a transient dimer with a lifetime so long that substantial deactivation would occur in the fused drops before fission. The models based on the fragmentation–coagulation or on the fusion–fission are therefore only crude approximations if the quenching process is represented by a stationary rate constant k_q.

Fluorescence quenching studies of intermicellar migration of reactants via coalescence-fragmentation reactions in micellar solutions in the presence of additives have been reported.[84,87,119] Time-resolved excimer formation of micelle-solubilized pyrene was used to investigate the intermicellar migration of pyrene in aqueous micelles.[84] It was observed that addition of medium-chain alcohols as well as electrolytes induces the coalescence–fragmentation reactions taking place on the pyrene excited-state time scale. However, the analysis of the quenching process considering the coalescence–fragmentation of the micelles has been performed on the basis of a model which assumes that the probe is an immobile species, i.e., the physical model underlying eq 20. In the case of fragmentation–coagulation process, k_+ is the second-order rate constant for the attachment of a fragment to a full-size micelle, and k_- is the first-order rate constant for the detachment of a fragment from a full-size micelle. Values of k_- in the range 0.1–3 μs^{-1} were determined in SDS in the concentration range 0.2–0.5 M and in the presence of added 1-pentanol up to 1 M. Moreover, the time scale at which fragmentation–coalescence is observed in the time-resolved fluorescence quenching experiments is much shorter than that at which the formation–breakdown process is observed when relaxation methods, such as T-jump method, are used. The proposed explanation for the difference was that the relaxation method gives an average over a series of sequential steps involved in the micelle formation–breakdown while time-resolved fluorescence measures only one step of that series and is therefore much faster than the whole process.[84]

At high surfactant concentration and in the presence of additives, errors can be introduced in the determination of aggregation numbers, quenching, and quencher exchange rate constants if intermicellar mobility of the excited probe is neglected. Furthermore, the excimer formation process used to probe the micellar system might have a inherent problem since this process can be reversible. A statistical model considering the dissociation of pyrene excimers in small micelles in the absence of reactant intermicellar exchange was reported by Infelta and Grätzel.[42] The rate constants for pyrene excimer formation and dissociation in micelles of sodium hexadecyltrioxyethylene sulfate were determined as $(9 \pm 1) \times 10^6$ and $(4 \pm 2) \times 10^6$ s^{-1}, respectively, showing clearly that the excimer dissociation is important.

The migration of long-chain alkylpyridinium quenchers was observed in sodium dodecyl sulfate upon addition of high concentration of 1-butanol.[87] Global analysis (vide infra) demonstrated that the exit rate constant of quenchers with different alkyl chain length is in this case identical. The quenching rate constant of 1-methylpyrene, k_q, and the exit rate constant of the quencher, k_-, as a function of the 1-butanol concentration are shown in Figure 8a. For concentrations of 1-butanol up to 1 M, k_q increases as a result of the reduction of the micellar size. The changes in the aggregation number of SDS upon addition of 1-butanol are shown in Figure 8b. If the concentration of 1-butanol exceeds 1 M, the k_q value drops, and in this concentration domain the quencher intermicellar mobility starts to be detected. Addition of more alcohol increases significantly the values of k_-. These results have been rationalized in terms of the coalescence–fragmentation model. The values of k_- found in this study were within the same time scale as those for the fragmentation rate constants reported by Malliaris et al.[83,84]

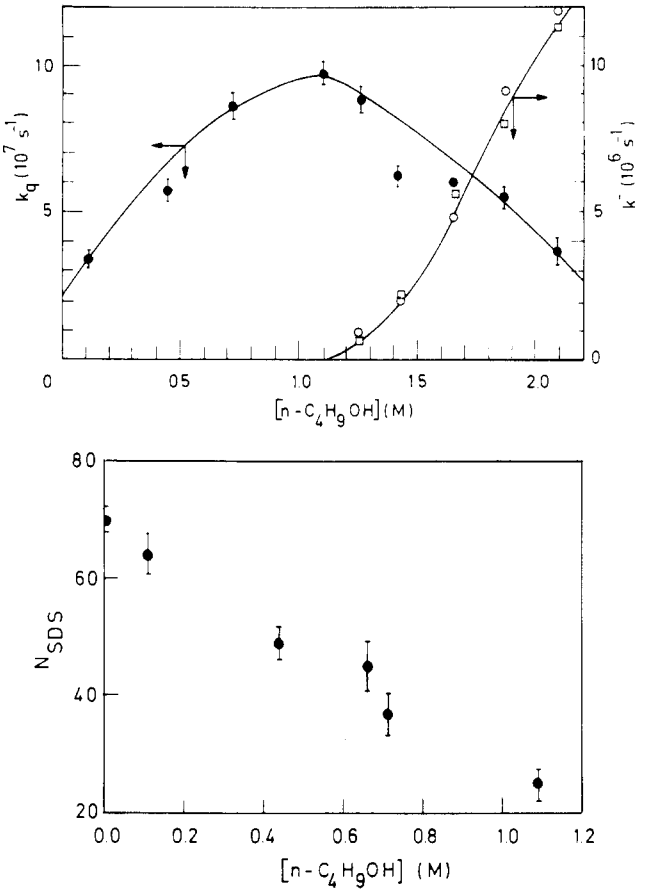

Figure 8. (a, top) Change of k_q (●) and k_- of $C_{10}PyCl$ (○), and k_- of $C_{14}PyCl$ (□) as a function of added 1-butanol concentration in 0.15 M SDS (from ref 87, copyright 1989, American Chemical Society). (b, bottom) Aggregation number of SDS micelles as a function of added 1-butanol, obtained by fluorescence quenching of 1-methylpyrene (from ref 87, copyright 1989, American Chemical Society).

The intermicellar exchange of solubilized reactants in reversed micelles or microemulsions has also been investigated by fluorescence quenching methods.[109–122] In contrast to the situation in aqueous micelle where the choice of a probe with a high hydrophobic character simplifies the quenching kinetics, the quenching process in reversed micelles and microemulsion is more likely to lead to a situation where the intermicellar mobility of both species is present particularly if fluorescent probes with a long-lived excited state are used. The other possible situations in relation to intermicellar mobility of the reactants are not excluded, but only a careful analysis of the experimental results can indicate what the appropriate model is for a given probe–

quencher–reverse micellar system. It is important to note that the choice of the probe/quencher combination is crucial for the successful use of the fluorescence quenching method to measure the size and the stability of reverse micellar aggregates.[115] In the study of reverse micelles of sodium bis(2-ethylhexyl)sulfosuccinate (AOT) in *n*-hexane at varying concentration of water, the best agreement between the aggregation numbers determined by the quenching method and those determined by ultracentrifugation were obtained with 1,4,6,9-pyrenetetrasulfonate (PTSA)/I^- as probe–quencher pair.[115] The short excited-state lifetime of this probe (≅10 ns) as well as the charge effect compelling the probe to the core of the water nanodroplet do not allow intermicellar exchange of PTSA during the time scale of the fluorescence quenching.

The first theoretical approach in reverse micelles including the intermicellar exchange of the excited probe into the framework of the quenching process was reported by Almgren et al.[49] They have pointed out that the fluorescence decay in a general case including the exchange of probe and quencher might still be described, as a good first approximation, by a similar decay function as that in eq 20 but with a generalized interpretation of the A_i parameters. They showed that the survival fractions of micelles containing one excited probe at time t is the solution of

$$df/dt = -k_0 f - k_q \langle x \rangle f \tag{34}$$

The fluorescence decay given by eq 28 is exponential if and only if $\langle x \rangle$, the average number of quencher in the subset of micelles containing the excited probe, is constant. If the decay has an exponential tail, then $\langle x \rangle$ has reached a stationary value indicated by $\langle x \rangle_s$. The time evolution of $\langle x \rangle$ from its initial value $\langle x \rangle = \bar{n}$ to this stationary value is governed by the following differential equation:

$$d\langle x \rangle/dt = -(\langle x^2 \rangle - \langle x \rangle^2)k_q + (k_- + k + k_t/2)(\bar{n} - \langle x \rangle) \tag{35}$$

The term in the first parentheses on the right-hand side of the equation is simply the variance of the quencher distribution. k_-, k, and k_t are the exit rate constant of quenchers from the micelle, the probe migration rate constant, and the fusion–fission rate constant, respectively.

It is a reasonable first approximation to assume that the variance is linearly related to the average. Under this condition, the fluorescence decay follows a Poisson decay law (eq 20) but with a generalized interpretation of the A_i parameters expressed as $\tilde{A}_i$ in

$$\tilde{A}_2 = k_q \langle x \rangle_s + k_0 \tag{36}$$

$$\tilde{A}_3 = \bar{n}(1 - \langle x \rangle_s/\bar{n})^2 \tag{37}$$

$$\tilde{A}_4 = k_q(1 - \langle x \rangle_s/\bar{n})^{-1} \tag{38}$$

Fitting of the fluorescence decay at sufficiently long times allows the determination of the model parameters k_0, k_q, and $\langle x \rangle_s/\bar{n}$. The relationship between $\langle x \rangle_s/\bar{n}$ and the rate parameters is obtained numerically. Almgren et al. applied this method in a study of quencher and probe transport in a microemulsion based on Triton X-100–toluene–water.[49] They considered only exchange by fusion–fission. Analysis of decay curves of the quenching process of ruthenium trisbipyridinium by methylviologen was used to investigate the probe and quencher intramicellar exchange as a function of the microemulsion composition. Increase of the surfactant concentration as well as the water percentage results in a faster intramicellar exchange of the solubilizates. The fusion–fission rate constant was found to be within the range (0.5–6) × 10^6 s^{-1}. The values of the self-diffusion coefficients of water, toluene, and Triton X-100 were also measured by the Fourier transform ^1H NMR pulsed-gradient spin-echo method. However, the fusion–fission process could not quantitatively explain the rapid self-diffusion of water observed in water-rich samples. It was suggested that for a high volume fraction of the dispersed phase, where the micelles are in a close spacing, a possible model explaining both types of experiments would be that the micellar compartments are transiently connected by narrow holes or channels, which rarely are large enough to permit quencher or probe to transfer but allow a rapid exchange of the small water molecules. In such a situation with close-packed micelles, the rate constant k_t should be visualized as an average frequency for the formation of channels allowing interdroplet exchange of probe and quencher. A similar model was considered to interpret the fast exchange of reactants solubilized in the reverse micelles of the system AOT/water/alkane.[121]

The study of droplet dynamics in microemulsions stabilized by non-ionic surfactants of the alkyl polyoxyether type by fluorescence quenching has been recently reported by Fletcher et al.[122] The interdroplet exchange of reactants was assumed to occur only by the fusion–fission mechanism as described above. Ruthenium trisbipyridinium and methylviologen were used as a probe and quencher, respectively. The interdroplet exchange rate constant was calculated on the basis of the Almgren approach. A linear relation between the first-order rate constant for reactant interdroplet exchange and the droplet concentration was observed, and a second-order rate constant interpreted as the rate constant for droplet coalescence was estimated. Its changes with surfactant and microemulsion composition were discussed in terms of the interdroplet interactions and the energies required to bend the surfactant monolayer and to desorb surfactant from the interface.

The problem of intermicellar exchange of reactants was subsequently treated by Tachiya.[50] The Laplace transform and the matrix formulation (the eigenvalues and eigenvectors problem) methods were applied in a numerical analysis of the probe migration and the fusion–fission process. Particularly, for the problem of probe migration, an analytical solution was obtained. The δ-response function was expressed as an exponential series:

$$f(t) = \exp[-k_0] \sum_{j=0} B_j \exp[-\beta_j t] \tag{39}$$

where the amplitudes are calculated by

$$B_j = \left[\sum_{n=0} \frac{\bar{n}^n}{n!} \exp[-\bar{n}]\left(\frac{k}{\alpha_j + nk_q + k}\right)^2\right]^{-1} \quad (40)$$

and α_j are the roots of

$$1 - kg(s) = 0 \quad (41)$$

with

$$g(s) = \exp[-\bar{n}]\sum_{n=0}^{\infty} \frac{\bar{n}^n}{n!(s + k + nk_q)} \quad (42)$$

which have to be obtained numerically. The decay rates $\beta_j = -\alpha_j$ and β_j are all positive. By comparison of the lowest eigenvalue and its amplitude with $\tilde{A}_2$ and exp$(-\tilde{A}_3)$, as given by eqs 36–37, it was demonstrated that the Almgren approximation remains valid only at a low average number of quenchers per micelle.[50]

Recently, a new methodology to investigate the fluorescence quenching in the presence of intramicellar exchange of probe and quencher has been introduced.[51,52,133,134] The migration dynamics of an excited probe is described by[50-52]

$$M^*_n + M_j \xrightarrow{k_p} M_n + M^*_j \quad (43)$$

where M^*_n denotes a micelle containing one excited probe and n quenchers, whereas M_j denotes a micelle with j quenchers but without an excited probe. k_p is the second-order rate constant for the probe migration process.

The δ-response function of the fluorescence decay in the presence of probe migration as well as in the general case where both probe and quencher exchange between micelles was obtained by using the integral equation formalism.[51,52] The fluorescence decay in the general case of monodisperse micelles is found by solving the following integral equation of the convolution type:

$$f(t) = kf(t) \otimes g(t) + g(t) \quad (44)$$

In eq 44, the convolution operator is denoted by $\otimes$. The initial function, $g(t)$, is simply the decay function in the case of mobile quencher–immobile probe (eq 20) multiplied by exp$[-kt]$. k if the first-order rate constant for intermicellar exchange of the probe defined as $k = k_p[M]$ or as the reciprocal of the first passage time between two micelles when migration through the aqueous phase is considered. Equation 44 can also be applied when no exchange of quencher occurs, but in this situation $g(t)$ is equal to eq 25 multiplied by exp$[-kt]$ as before.

The solution of eq 44 may be obtained by the method of successive approximations. Applying this procedure, the following von Neumann type series is generated:

$$f(t) = g(t) + kg(t) \otimes g(t) + k^2 g(t) \otimes g(t) \otimes g(t) + \ldots \quad (45)$$

The first term on the right-hand side of eq 45 is the survival fraction of probes which at a time t has not yet migrated, the next term represents the survival fraction which has migrated once and, and so on.

Since eq 44 is an integral equation of the convolution type, it can be solved by Fourier or Laplace transform. Defining the correspondent unitary transformation as U, the solution of eq 44 is given by the following expression involving the inverse of the unitary transformation:

$$f(t) = U^{-1}\{\hat{g}(s)/(1 - k\hat{g}(s))\} \quad (46)$$

The Laplace transform is appropriate for evaluating the relative fluorescence intensity in the absence and presence of added quencher, I_0/I, observed using continuous excitation. Defining $\hat{f}(s)$ and $\hat{g}(s)$ as the Laplace transform of $f(t)$ and $g(t)$, respectively, one has

$$\hat{f}(s) = \hat{g}(s)(1 - k\hat{g}(s))^{-1} \quad (47)$$

where

$$\hat{g}(s) = \exp[-\mu]\sum_{i=0}^{\infty} \frac{\mu^i}{i!(s + \gamma + i(k_q + k_{exq}))} \quad (48)$$

$$\mu = \frac{\bar{n}k_q^2}{(k_q + k_{exq})^2} \quad (49)$$

$$\gamma = k_0 + k + \frac{\bar{n}k_q k_{exq}}{(k_q + k_{exq})} \quad (50)$$

Considering that $\hat{f}(s)$ satisfies the conditions imposed by the final value theorem, then

$$I_0/I = \tau_0/\int_0^\infty f(t)\,dt = \tau_0/\lim_{s\to 0} \hat{f}(s) = \tau_0[\hat{g}(0)^{-1} - k] \quad (51)$$

In the limit of fast probe migration compared to the other processes $\hat{g}(0)^{-1} \approx k + k_0 + \bar{n}k_q$, and the stationary intensity ratio turns into a linear Stern–Volmer relation:[134b]

$$I_0/I = 1 + \tau_0 k_q \bar{n} \quad (52)$$

If the quenching process is slowed down for instance due to the presence of a higher activation energy barrier, then the situation where $k \gg k_q$ is likely to occur. In such case no information about molecular exchange of the reactant can be obtained by the analysis of the fluorescence decay ($f(t) \approx \exp[-(k_0 + \bar{n}k_q)t]$) or from stationary measurements. The same limits are attained if $k_{exq} \gg k_q$.

From the analysis of the series in eq 45, it was possible to derive an approximate solution to the fluorescence decay in this general case.[133] On the basis of the Almgren approach, it was shown that the average number of quenchers in the subset of micelles that still contain the excited probe, $\langle x\rangle_s$, can be evaluated by the following expression:

$$\langle x\rangle_s = \left(\frac{k}{k_q}\right)\left\{1 - \exp\left[-\frac{A_3A_4}{(A_4 + k)}\right]\right\} + \frac{\bar{n}k_{exq}}{A_4} \quad (53)$$

Figure 9 shows the variation of $\langle x\rangle_s$ as a function of the logarithm of the ratio of the exchange rates and the quenching rate constant at different values of $\bar{n}$. The points account for the values calculated by the iterative method suggested by Almgren,[49] while the lines represent the values obtained from eq 53. In Figure 10 the exact δ-response function is compared with the approximate solution based on eq 20 and in the set of relations for the generalized $\tilde{A}_i$ parameters as given by eqs 36–38. It can be seen that the approximate solution describes adequately the initial part of the decay, but at long times deviations from the numerical values are

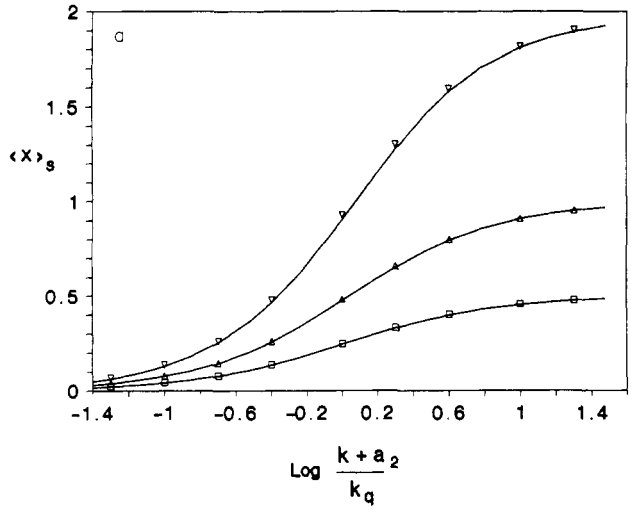

Figure 9. Stationary-state average number of quenchers in the subset of micelles with one excited probe as a function of the ratio of the exchange rate constants and the quenching rate constant in the case of mobile quencher–mobile probe for different initial quencher occupancy: (□) $\bar{n}$ = 0.5; (△) $\bar{n}$ = 1.0, (▽) $\bar{n}$ = 2.0 (from ref 133, copyright 1992, American Chemical Society).

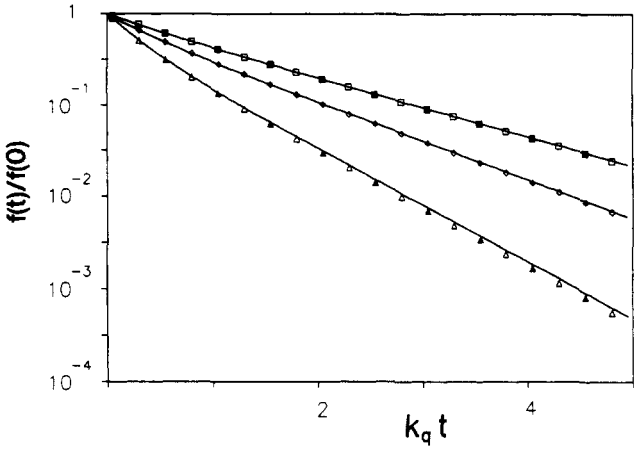

Figure 10. Normalized fluorescence decay in the case of both probe and quencher as mobile species with $k = k_{exq} = k_q/2$. Full lines correspond to the approximate solution. The closed symbols represent the numerical values from the integral series expansion (eq 45) with five to eight terms while the open symbols are the values from the numerical solution of the system of differential equations (eq 9 in ref 52) (from ref 133, copyright 1992, American Chemical Society).

observed and a good fit is obtained only in the case of low $\bar{n}$ values. The quenching process of sodium 1-pyrene sulfonate by tetradecylpyridinium chloride in CTAC micelles was recently studied considering probe migration.[134a] Simultaneous analysis of several decay traces at different quencher concentrations demonstrated that the pyrene sulfonate ion is a mobile species while the quencher remains immobile during the time window of the fluorescence event. Figure 11 shows the observed values of the probe migration rate constant as a function of the micelle concentration. The observed linear relation between the probe migration rate constant and the micelle concentration yielded an apparent second-order rate constant of (3.0 ± 0.4) × 10^9 mol^{-1} L s^{-1}.

The exponential series expansion solution originally introduced by Tachiya[50] in the case of probe migration was recently extended to the case of quencher and probe

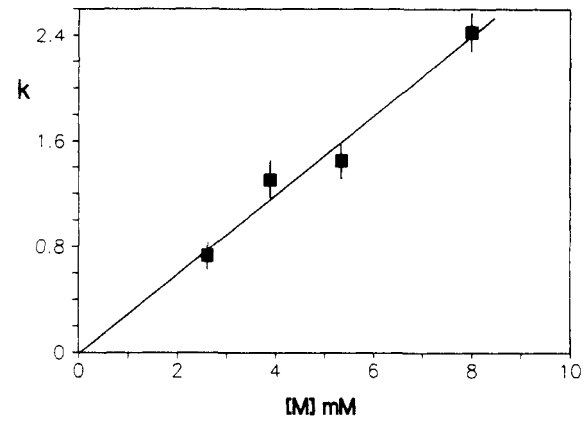

Figure 11. Intermicellar probe migration rate constant (k, μs^{-1}) as a function of the micellar concentration (from ref 134a, copyright 1992, American Chemical Society).

exchange.[54] The decay function $f(t)$ is expressed as an exponential series:

$$f(t) = \sum_{j=0} B_j \exp[-\beta_j t] \tag{54}$$

in which the amplitudes B_j are equal to

$$B_j^{-1} = \exp[-\mu] \sum_{n=0} \frac{\mu^n}{n!} \left(\frac{k}{\alpha_j + \gamma + n(k_q + k_{exq})} \right)^2 \tag{55}$$

where α_j represents the roots of eq 41 but with $\hat{g}(s)$ given by eq 48. The decay constants $\beta_j = -\alpha_j$ and all B_j are positive. The parameters μ and γ are defined by eqs 49 and 50, respectively.

II.2.3. Factors Affecting the Quenching Process

(a) *Effect of Micelle Polydispersity.* In all previous discussions, the fluorescence quenching process has been analyzed considering micelles as monodisperse. This assumption will be valid as long as the micellar size distribution remains narrow. However, it is well documented that ionic micelles in the aqueous phase are susceptible to growth when salt is added to the solution.[79,83,84,137] In some systems, micellar shape changes are observed upon addition of salt.[169,170] In the case of non-ionic micelles, an increase in size of the micelle with temperature has been observed and attributed to changes in the water hydrating shell of the polar head groups of the nonionic micelle.[135,136]

In each case, the increase of the micellar size is usually associated with a broadening of the micellar size distribution. Polydispersity is likely to be present also in reverse micellar systems and in microemulsions.[138,139] The solubilization process of the probe and quencher then becomes size dependent. There will be a higher probability of finding a hydrophobic probe and quencher pair in a larger aqueous micelle than in a smaller one. Since probe concentration is usually much lower than the total micelle concentration, the quenching process selects a subset which is shifted toward the fraction of larger micelles. As long as more quencher is added, the balance between particle number and size effects will force the quencher to be distributed along the whole fractions of the micellar sizes. As a result, the experimentally estimated aggregation number and the quenching rate constant obtained by considering the system as monodisperse may be a function of the quencher concentration.

Polydispersity effects on fluorescence quenching were originally studied by Almgren and Löfroth.[140] Two extreme cases were considered: a static one, where no size changes of the micelles occurs during the residence time of the reactants, and a dynamic one where very large size variations take place. Analysis of simulated decays assuming Gaussian and exponential micellar size distributions showed that in the static case, the estimated aggregation number will decrease with quencher concentration from the weight average number in the limit of zero quencher concentration. In the dynamic case, the number average aggregation number is obtained independent of quencher concentration.

The theory of a polydispersity-assisted quenching process was later extended by Warr and Grieser to steady-state and time-resolved experiments.[144] In the absence of exchange of probe and quencher during the fluorescence event, the measured average aggregation number referred to as the apparent average aggregation number, obtained by using eq 25, is related to the quencher concentration as follows:

$$N_{agg} = N_w - \frac{\sigma q}{2} + \frac{\xi q^2}{6} - \dots \quad (56)$$

where N_w is the weight average aggregation number and σ and ξ are the second and third cumulants of the micellar size distribution. q is the ratio of quencher to surfactant molecules in the aggregates. If solubilization of quencher molecules should not perturb the micellar structure only a small fraction of q space will be experimentally accessible. Quasi-monodisperse systems should show no change of N_{agg} with q; a linear dependence of N_{agg} with q indicates that the distribution is symmetrical, and a nonlinear one, that the distribution is skewed. The polydispersity of several micellar systems has been investigated on the basis of the discussed model.[135,140-145]

(*b*) *Deviations from the Poisson Distribution.* The solubilization of probe and quencher are usually assumed to be independent processes. A Poisson distribution is then realized as long as the average occupancies are relatively low. When a maximum number of quenchers per micelles, say m, due to size restriction is admitted, the distribution of quencher among the micelles becomes binomial:[146,147]

$$B_n = \binom{m}{n}\left(\frac{\bar{n}}{m}\right)^n\left(1 - \frac{\bar{n}}{m}\right)^{m-n} \quad (57)$$

Mathematical expressions of the fluorescence decay in the case of a binomial distribution of quencher were derived by Tachiya.[47] Nakamura et al. reported that the fluorescence quenching of pyrene by Cu^{2+} and Eu^{3+} in SDS micelles may be described by a binomial distribution of decay rates.[148] They concluded that the maximum number of those ions per SDS micelle is about 4. This result contrast with previous investigations of the same system where Poisson distribution was successfully applied. Also the low value of the maximum number of quenchers seems to be underestimated. Experimentally it is always possible to control the quencher concentration in order to have an average occupancy ≤ 2 where Poisson distribution holds. Also, the quencher can be a surfactant-like molecule, so that its presence in less than 5% of the surfactant monomer number will not disturb the micelle structure if the quencher molecule has a size similar to that of the surfactant molecule. On the other hand, functionalized probes with a large chromophore and a long alkyl chain do affect the micellar structure.[149] A similar approach has been made in other systems, e.g., the nonexponential decay of the excited state of $Ru(bipy)_3^{2+}$ adsorbed on clays containing quenching impurities (Fe^{3+}) was described by a binomial distribution of decay rates.[150] The probe and quencher were considered immobile species, and the binomial distribution was related to the interplay between the excited probe site and the nearest lattice sites of the solid which may be occupied by the quencher ions.

(*c*) *Nonideality in the Probe Quencher Distribution Due to Intramicellar Probe–Quencher Complexation.* When the probe in the ground state can form a complex with the quencher, the distribution of both species is no longer independent. The fraction of micelles containing the probe will be occupied with a slightly higher probability than that without probe. Considering that the fluorescence quenching method selects only the fraction of micelle containing an excited probe, the experimentally determined quencher occupancy $\bar{n}$ may not be strictly the ensemble average. If the probe quencher association leads to a nonfluorescent complex, substantial differences between the time-resolved and stationary measurements could occur because the former method relates only to that fraction of probes which acts through a dynamic quenching process while in the latter one both dynamic and static quenching contribution are measured.[151-153] It has been demonstrated that the fluorescence quenching of pyrene by *N,N'*-dimethyl-4,4'-bipyridinium dichloride has static and dynamic contributions.[151a] Ground-state charge-transfer complexes between anthracene or 1,4-dimethylnaphthalene and arene diazonium salts were observed in SDS micelles.[152] A kinetic scheme considering both static and dynamic contributions was formulated to explain the quenching data.

II.3. Energy Transfer in Micelles

Energy transfer between donor and acceptor solubilized in micelles has been used to investigate micellar solutions.[154-167] The distance dependence of the probability of dipolar electronic energy transfer was used to study the spatial distribution of the donor–acceptor pair in the host micelle structure and to derive information on molecule–micelle interaction. Similar issues are also very important in the investigation of sensitized fluorescence or of photochemical processes in natural and artificial systems based on molecular aggregates.

Experimentally, the fluorescence decay of the donor is monitored. If a Förster dipole–dipole mechanism in the limit of dynamic regime is assumed, then the fluorescence δ-response function of the donor population in the presence of Poisson distributed acceptor with an average occupancy $\bar{n}$, is given by[166,167]

$$\rho(t) = \exp[(-t/\tau_0) - \bar{n}(1 - J)] \quad (58)$$

where

$$J = \int h(r) \exp[-(R_0/r)^6(t/\tau_0)]\, dr \quad (59)$$

with $h(r)$ the distance distribution function for the

donor–acceptor pair. τ_0 and R_0 are the donor decay time in the absence of acceptors and the so-called Förster radius which corresponds to the distance where the energy transfer probability equals the emission probability, respectively. Micellar structural details are then related to the decay profile via $h(r)$. However, if R_0 is larger than the micellar diameter but still smaller than the average distance between micelles, than the decay will be only slightly affected by the spatial distribution of donor and acceptor in the same micelle, $J \cong 0$, and the fluorescence decay becomes single exponential with a decay time τ_0 and amplitude equal to $\exp[-\bar{n}]$.

Different models where specific forms of $h(r)$ are assumed, have been formulated.[162-164,166,167] The detailed description of those models is outside of the scope of the present review, but some of the experimental finding are briefly discussed. Recently, Berberan-Santos et al. analyzed time-resolved quenching of several different donor–acceptor pairs in SDS micelles.[167] The decay profiles could not be completely explained by four models in which orientational dynamics and uncorrelated spatial distributions for the donor–acceptor pair are varied. The deviations were then rationalized on the basis of probe-induced perturbations of the micelle structure resulting in a closer-than-random distance distribution. However, if correlation between the probe molecules inside the micelle occurs, then the solubilization process is no longer independent and eq 58 should be modified.[166b] Another factor usually missing in the models is the effect of the micellar polydispersity. If one assumes an average micelle radius, it seems that the donor fluorescence decay, which has a sharp dependence on the micelle radius, is preaveraged over the ensemble, and the decay is not considered as a result of quenching in different micelle subsets in which size as well as quencher occupancy is not constant. The problem that one faces is similar to that of a diffusion controlled quenching when the size distribution is not narrow.

II.4. Quenching Process in Cylindrical Micelles

Changes in the micellar form upon addition of salt and cosurfactant and at a higher surfactant concentration is likely to occur in several systems.[14] For instance, CTAC micelles are susceptible to a transition from spheres to cylinders upon exchange of a chloride counterion by chlorate;[169,170] SDS micelles are reported to be nonspherical at a higher sodium chloride concentration. For nonionic micelles, a high aggregation number and nonspherical micelles are predicted. For these aggregates, the most favored configuration seems to be a prolate ellipsoid (rod).[14a] Hatlee et al.[33] suggested that the sphere–rod transition would influence the rate of intramicellar reactions by changing the dimensionality of the diffusion space. In an extreme situation where large micelles are present, the models based on small and monodisperse micelles may not be valid due to the approximately continuous quencher number density in the reaction volume and/or due to the considerable amplitude of the diffusion transient.

The problem of fluorescence quenching in large micelles has been formulated on the basis of the diffusion equation of free particles in a finite or semi-infinite cylinder as a geometric model for rodlike micelles.[168-170] Van der Auweraer et al.[168] considered the quenching process as taking place on the surface of a cylinder of length L and radius R_c. The probe is assumed to remain immobile in the middle part of the cylinder. This sector of the cylinder forms a reaction zone with an average rate constant, $\langle k \rangle_{perp}$, given by

$$\langle k \rangle_{perp} = \frac{3D_c\pi R_c}{(\pi R_c - R_{pq})} \tag{60}$$

This approximation allows introduction of a radiating boundary condition at $2L - R_{pq}$ and at R_{pq} with a rate constant equal to $R_{pq}\langle k \rangle_{perp}$. R_{pq} is the sum of the probe and quencher molecular radius, and D_c is the mutual diffusion coefficient in the medium. The equatorial diffusion is then decoupled from the axial diffusion. The problem becomes analogous to that of the average temperature of a slab with thickness $2L$ radiating at both ends in a medium at zero temperature and having an initial temperature $^1/_2L$. The space average concentration of excited probe–quencher pair is then

$$\langle p \rangle_{cyl} = lL\sum_{n=1}^{\infty}\frac{\exp[-\Gamma_n^2 D_c t/L^2]}{\Gamma_n^2(L^2l^2 + Ll + \Gamma_n^2)} \tag{61}$$

where Γ_n is the solution of

$$\tan \Gamma_n = lL/\Gamma_n \tag{62}$$

with

$$l = R_{pq}\langle k \rangle_{perp}/D_c \tag{63}$$

The fluorescence decay of an ensemble of micelles containing statistically independent quenchers, which are distributed over the micelles according to a Poisson distribution, is

$$f(t) = \exp[-k_0 + \bar{n}(\langle p \rangle_{cyl} - 1)] \tag{64}$$

It has been shown that diffusional transients will only lead to important deviations of the experimentally determined decay from the decay expected on the basis of eq 25 when a short-living probe ($\tau_0 < 50$ ns) is used in larger micelles ($L > 400$ Å or $N_{agg} > 400$). In addition, for a small aggregation number (corresponding to $L/R_c < 2\pi$) it will be difficult to determine from the experimentally observed data whether the model for spherical or the model for cylindrical micelles is most adequate.[168]

Fluorescence quenching in rodlike micelles was also studied by Almgren et al.[169,170] They proposed a model for a quenching process in semi-infinite cylinders. In that model, the excited probe is assumed to be fixed at the bottom ($x = 0$) of an infinitely long cylinder of radius R_c, and the quenchers initially form a constant number density along that axis, $c(x,t=0)$. A reaction zone with a finite rate constant k_q is defined to represent the quenching process in the vicinity of the excited probe. In such approximation, the problem is then converted to a unidimensional diffusion in a semi-infinite medium with radiation boundary condition. The resulting expression for the fluorescence decay is

$$\ln\left(\frac{f(t)}{f(0)}\right) = -k_0 - \frac{2C_0}{\nu}\left[\exp[\nu^2 D_c t]\ \mathrm{erfc}\ (\nu(D_c t)^{1/2}) - 1 + \frac{2\nu(D_c t)^{1/2}}{\pi^{1/2}}\right] \tag{65}$$

where

$$\nu = 2k_q R_c / 3D_c \quad (66)$$

Experimental results obtained in the quenching of pyrene by benzophenone in CTAC micelles in the presence of moderate amount of sodium chlorate was chosen to investigate the quenching process. The formation of rodlike micelles upon addition of sodium perchlorate was confirmed from viscosity measurements. Decay curves for different quencher concentrations were fitted with eq 65 in a global analysis (vide infra). A good global fit was obtained with better local statistical parameters for the curves at lower quencher concentration. From the results, the values of $k_q = 2.4 \times 10^7$ s^{-1} and $D_c = 9 \times 10^{-1}$ m^2 s^{-1} were calculated on the basis of an assumed radius of 21 Å for the cylindrical micelles. A general situation where the quencher migrates between micelles throughout the aqueous phase was also introduced. The model was later used to interpret the deactivation of long-lived probes such as triplet states. The mutual diffusion coefficient of the probe and quencher, D_c, as well as the quenching rate constant, k_q, could be estimated.[170a]

II.5. Dispersive Kinetics and Fractal Decay Law

The fluorescence quenching in microheterogeneous systems can be affected not only by the statistical distribution of quenchers but also by factors such as structural and energetic disorder of the system. In the last few years a fractal approach to describe the relaxation process of an excited probe in disordered materials has been considered.[171] A decay law which has been often used in the analysis of experimental data is the stretched exponential

$$f(t) = \exp[(-t/\tau)^\beta] \quad 0 < \beta \leq 1 \quad (67)$$

The exponent β and the time constant τ depend on the system and on the microscopic relaxation process. Stretched exponential decays appear in various studies of dynamic process such as NMR, direct energy transfer and diffusion controlled processes in restricted geometries or low dimensional systems. Equation 67 expresses the relationship between structural properties and dynamics. It is of fundamental importance in the study of molecular transport in porous solids and glasses.[171]

The direct energy transfer (DET) from an excited donor to acceptors randomly distributed on fractals and the indirect energy transfer (IET), which could involve energy migration over the donor subsystem or molecular self-diffusion of the acceptor in a fractal structure where the donor is a static target, are two distinct classes for which the relaxation process results in a stretched exponential decay.[171] The main difference between these two classes is that DET depends on the density of sites around the donor which could eventually be occupied by acceptor, a parameter which scales with the geometrical fractal dimension of the medium. On the other hand, IET depends on the topology of the random walk of the exciton migration or self diffusion of the quencher in the target problem (i.e., the dynamic connectivity of the system). For direct energy transfer on a fractal

$$f(t) = \exp\left[-\left(\frac{t}{\tau_0}\right) - \frac{pdB}{\tilde{d}}\Gamma\left(1 - \frac{\tilde{d}}{6}\right)\left(\frac{t}{\tau_0}\right)^{\tilde{d}/6}\right] \quad (68)$$

is the decay function where τ_0 is the fluorescence lifetime of the donor in the absence of acceptors, $\tilde{d}$ is the fractal dimension, p is the probability with which acceptors occupy sites in the fractal structure and B is a time-independent factor. When the IET process is considered, one has

$$f(t) = \exp\left[-\left(\frac{t}{\tau_0}\right) - a\sigma\left(\frac{t}{\bar{\tau}}\right)^{\tilde{d}/2} + \frac{b\sigma^2}{2}\left(\frac{t}{\bar{\tau}}\right)^{\tilde{d}}\right] \quad (69)$$

where $\bar{\tau}$ is the average time of the energy migration process, $\sigma = -\ln(1-p)$, a and b are time-independent factors, and $\tilde{d}$ is the spectral dimension or fracton. If the target problem is considered, then b in eq 69 is zero, and the decay due to quenching is a single stretched exponential valid over the whole time range contrary to the situation where b is a positive constant.

Equation 68 was used by Mataga et al.[172] to interpret the energy transfer of rhodamine 6G to malachite green when both dyes are adsorbed on the surface of a DHP vesicle. The fractal dimension $\tilde{d}$ was attributed to the acceptor spatial distribution on the vesicle surface. However, when the energy migration among cationic porphyrins adsorbed on the surface of DPH vesicles was studied, the quenching due to energy trapping by dimers and higher porphyrin aggregates was interpreted as an IET process.[173] Analysis of fluorescence decay curves with eq 69 at several different concentrations of DHP has yielded $\tilde{d} = 1.65$.

Fluorescence probing of bimolecular reactions on lipid vesicles was also investigated by several authors using the framework of fractal dimension. In the study of self-quenching of excited pyrene in small unilamelar vesicles of dipalmitoylphosphatidylglycerol, Argyrakis et al.[174] suggested that the quenching process could be well interpreted on the basis of a fractal decay (eq 67). However, they noted that the spectral dimension, $\tilde{d}$, was a function of the pyrene concentration particularly at low lipid concentration. Considering that the theory does not predict a dependence of $\tilde{d}$ with the concentration of traps (in that case the ground-state pyrene molecules), the unexpected decrease of $\tilde{d}$ with increasing pyrene concentration was ascribed to a quasi-static quenching at a high pyrene concentration. A steeper decrease of the decay profile due to the quasi-static contribution leads the $\tilde{d}$ values to appear smaller in order to account to this effect. However, excimer formation in vesicles has been treated as a bicompartmental system (two-state process) with a well-defined quenching mechanism where the backward step of the excimer kinetic is considered.[175] The theory underlying eq 69 assumes the quenching process to occur at the first encounter of the excited probe with the trap and a dissociation process is not considered.

Fractal modeling of fluorescence quenching has been tentatively used to explain the quenching mechanism in systems like small aqueous micelles, reverse micelles and microemulsions.[176] However, this new approach has not yet been as systematically tested using simultaneous analysis of the decay surfaces as the stochastic approach, described in II.2, has been. Also the information provided by fitting decays in micellar solution with a fractal decay law neither allows size characterization nor quantitative evaluations of intermicellar exchange rate constants. If micellar clusters are formed, as occurs in microemulsions above the percolation threshold, then the quenching process becomes a

function of the micelle connectivity, and fractal decay theory may be more properly used.

III. Analysis of Fluorescence Decay Data in Micelles

III.1. Reference Convolution Method[177-182]

Time-resolved fluorescence quenching in micelles can be properly measured by a time-correlated single-photon-counting technique. The use of a stable mode-locked ion or Nd:Yag laser to pump a tuneable dye laser producing very short pulses at a high repetition rate and fast timing detection has much increased the quality of the counting data. Besides the Poisson noise inherent to the counting technique, systematic errors may be also present in a sample decay. Systematic error from drift in the excitation source and electronics, detector dark counts, pulse pileup, or rf noise may also distort the data. Proper management of systematic and random errors is then essential in instrumental design and in the data analysis procedure.[183]

In the above sections, models for fluorescence quenching in micelles have been discussed and in several cases the sample response function of the system, $f_s(t)$, which corresponds to a decay after a δ-pulse excitation has been derived. In an ideal time-correlated single-photon-counting experiment, the time-resolved fluorescence profile of the sample, $d_s(\lambda_{ex},\lambda_{em},t)$, obtained by excitation at wavelength λ_{ex} and observed at emission wavelength λ_{em}, is the convolution product of the instrument response function irf $(\lambda_{ex},\lambda_{em},t)$ and the true sample response function $f_s(\lambda_{ex},\lambda_{em},t)$:

$$d_s(\lambda_{ex},\lambda_{em},t) = \text{irf}\,(\lambda_{ex},\lambda_{em},t) \otimes f_s(\lambda_{ex},\lambda_{em},t) \quad (70)$$

Usually, the experimentally determined functions irf $(\lambda_{ex},\lambda_{ex},t)$ and/or irf $(\lambda_{em},\lambda_{em},t)$ will differ from irf $(\lambda_{ex},\lambda_{em},t)$ due to the wavelength dependence of the instrument response. Their use in the model-fitting calculation can lead to inaccurate results. The best method to correct for this wavelength variation of the instrument response function is the reference convolution method.[177-182] In the reference convolution method, eq 70 is replaced by

$$d_s(\lambda_{ex},\lambda_{em},t) = d_r(\lambda_{ex},\lambda_{em},t) \otimes \tilde{f}_s(\lambda_{ex},\lambda_{em},t) \quad (71)$$

In eq 71, $d_r(\lambda_{ex},\lambda_{em},t)$ is the decay of a reference compound measured at the same instrumental settings as used for the sample and $\tilde{f}_s(\lambda_{ex},\lambda_{em},t)$ is the modified sample response function. It has been shown[179-182] that if the fluorescence δ-response function of the reference compound is monoexponential:

$$f_r(t) = a_r \exp[-t/\tau_r] \quad (72)$$

where τ_r denotes the decay time of the reference compound and a_r the corresponding scaling factor, $\tilde{f}_s(t)$ satisfying eq 71 is

$$\tilde{f}_s(t) = a_r^{-1}[f(0)\,\delta(t) + f'_s(t) + f_s(t)/\tau_r] \quad (73)$$

where $\delta(t)$ is the Dirac delta function and $f'_s(t)$ denotes the time derivative. For example, considering the four-parameter equation in micelle quenching kinetics as that given in eq 20, the following modified sample response function can be written:[85]

$$\tilde{f}_s(t) = a_1\{\delta(t) + (\tau_r^{-1} - A_2 - A_3A_4 \exp[-A_4t]f(t))/A_1\} \quad (74)$$

Estimates of model parameters are usually computed by nonlinear weighted least-squares fitting based on Marquardt algorithm.[184] Error estimates on the model parameters and a statistical measure of goodness-of-fit are essential points in the data analysis.[183] After fitting to a model function, a careful inspection of the differences between observed and fitted data should be worked out. This residual analysis usually comprehends the calculation of the reduced χ^2 and its normal deviate.[181b,183] Graphical methods such as weighted residual plots and the autocorrelation function are very useful for observing patterns in the data which can reveal appropriateness or lack-of-fit of the proposed model.[185] The Durbin–Watson parameter[186] to test for serial correlation between residuals, the run test[187] to examine the randomness of the time sequence of the residuals, and the percentage of the residuals within the [2,–2] interval are also additional numerical statistical tests which make the residual analysis more reliable.

Because of the intrinsic complexity of the micelle quenching models and their usually high number of fitting parameters, successful results with simulated data represent to the experimenter a unique way for delimiting the boundaries for a safe use of quenching methods in the study of micelles. Typically, synthetic decay data can be generated by numerical convolution of a nonsmoothed instrumental response function, such as an experimental lamp or laser pulse profile, with an assumed δ-response function of desired parameters, followed by addition of Gaussian or Poisson noise depending of the number of counts in a given channel.[181a] The analysis of simulated or synthetic decays of the fluorescence quenching in micelles by standard deconvolution techniques offers the possibility of investigating several points such as model appropriateness and accuracy of recovered model parameters and the possibility of discriminating between competing models. Two of the current methodologies in data analysis of micelle quenching are now discussed. Their use in simulated as well as real data is illustrated.

III.2. Global Analysis in Micelle Quenching Kinetics

Decay curves observed in micelle quenching kinetics may be collected at different experimental conditions (quencher or micelle concentration, wavelength, etc.). In single-curve analysis, the individual decay curves are analyzed separately to obtain decay parameters. Although this procedure can be adequate in many cases, it fails to take full advantage of the relationships that may exist between individual curves. The simultaneous analysis of related fluorescence decay experiments exploits these relationships between decay curves by linking common model parameters in the analysis. This approach has been called global analysis of decay surfaces.[188-192] It has been applied to a number of problems including fluorescence quenching in micelles. To illustrate its application, let's consider the fluorescence quenching model for immobile probe and quencher. If decay curves at different quencher concentrations are collected, then the decay rate constant of the probe

in absence of quencher, k_0, the micellar concentration, [M], as well as the quenching rate constant, k_q, may be linked because these model parameters are independent of the quencher concentration. Considering eq 25 a feasible model linking scheme in global analysis can be represented as in Scheme I. It has been demonstrated

Scheme I

1	k_0			τ_r
2	k_0	k_q	$[Q]_1/[M]$	τ_r
3	k_0	k_q	$[Q]_2/[M]$	τ_r
.	.	.	.	.
.	.	.	.	.
.	.	.	.	.
i	k_0	k_q	$[Q]_i/[M]$	τ_r

(75)

that such a procedure results in a superior recovery of model parameters than single curve analysis.[85] Also the inclusion of a sample decay with no added quencher (corresponding to sample 1 in the scheme above) and the linking of the probe's decay rate constant is a pertinent test of the assumed monoexponential decay of the probe in the absence of added quencher leading to a better determination of the model parameters. The quenching of 1-methylpyrene by tetradecylpyridinium chloride in DTAC micelles was reinvestigated by this approach.[85] Excellent agreement with previously reported values of quenching rate constant and average aggregation number in single curve analysis were obtained. The recovered decay parameter k_0, [M], k_q from simultaneous analysis of six curves at different quencher concentrations are given in Figure 12. Each individual curve analysis also resulted in satisfactory fits. However, the parameters recovered by single curve analysis are scattered around the "global" values. With global analysis similar trends in the parameter recovery were obtained in the analysis of the fluorescence quenching, with the same probe–quencher pair, in SDS aqueous micelles.[85b] Simultaneous analysis has been also applied to investigate the micelle quenching process in the presence of mobile quenchers (eq 20).[86] Analysis of synthetic decay data was used to determine the optimal experimental conditions to the number of data channels (time window), quencher concentration range and number of experiments in the global analysis. The results indicated that at least $^1/_4$K data points per curve are needed for recovering parameters and the larger the time window, the more accurate the model parameters become. It was demonstrated that the quencher concentration has no influence on the accuracy of the estimated parameters. Moreover, an increase in the number of analyzed curves resulted in better accuracy. The applicability of this simultaneous analysis approach was extended to real experimental data obtained from the quenching of 1-methylpyrene by the mobile quencher *m*-dicyanobenzene in SDS.[86] The same approach was used successfully in the analysis of the quenching process of this same probe by alkylpyridinium chlorides in cationic as well as anionic micelles in the presence of added butanol[87] as discussed early.

Simultaneous analysis is a powerful method to investigate probe and quencher intermicellar exchange.[49,134] If reaction exchange in microemulsions is

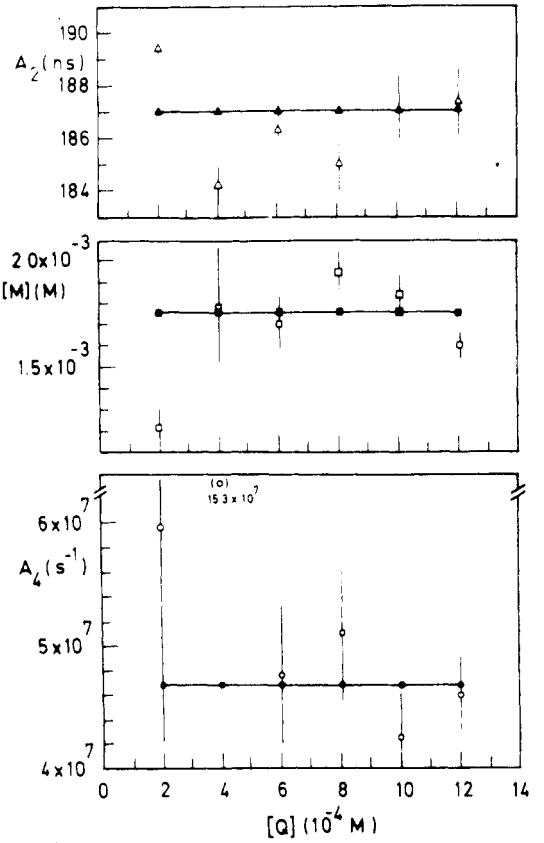

Figure 12. Estimated decay variables A_2 (△, ▲), [M] (□, ■) and A_4 (○, ●) from statistically acceptable single (open symbols) and multiple (horizontal lines with filled symbols) curve analyses of the fluorescence decays of 1-methylpyrene quenched by *N*-tetradecylpyridinium chloride in DTAC micelles according to eq 20 plotted versus [Q] (from ref 85, copyright 1988, American Institute of Physics).

analyzed on the basis of the Almgren approach considering the fusion–fission process, then the parameters k_0, [M], and k_q can be linked. However, $\langle x \rangle_s$ cannot be linked due to its dependence on the quencher concentration. Thus the fusion–fission rate constant should be determined indirectly. On the other hand, if exchange of probe and quencher is described by the probe migration model in its general formulation, then whole linking of the model parameters in global analysis is possible.[134] A particular case, where only the probe migrates between micelles, was recently investigated using the simultaneous analysis of the decay surface. The accuracy of recovery decay parameters (k_0, [M], k_q, and k) was superior in simultaneous analysis of several decays at different quencher concentrations than that of the single-curve analysis. Global analysis was superior in recovering model parameters even when the sum of the counts of the samples had practically the same total number of counts as the samples analyzed individually. Also, the standard deviations of the recovery parameters were smaller in global analysis than those obtained with individual analysis of samples.

However, the results from the analysis of synthetic data indicated that no model discrimination between mobile and immobile probe on the basis of fitting criteria is possible when the probe migration rate constant is much smaller than the quenching rate constant and the reciprocal of the decay time in the absence of quencher as well. Nevertheless, the model discrimination was possible on the basis of systematic analysis

of parameter recovery. The global approach was then used to investigate the mobility of the ionic probe sodium 1-pyrene sulfonate in CTAC micelles during the quenching process by the immobile quencher tetradecylpyridinium chloride. The experimental results indicated that PSA is a mobile probe in CTAC. Analysis of the system where the PSA was replaced by 1-methylpyrene confirmed that this more hydrophobic probe does not migrate between micelles during its excited-state lifetime. In the study of fluorescence quenching of PSA by hexadecylpyridinium chloride in poly(vinyl alcohol) in the presence of added CTAC, the formation of polymer supported micelles was investigated on the basis of global analysis. The results indicated mobility of PSA between micelles supported in the same polymer chain.[131]

The general fluorescence quenching model in monodisperse micelles where intermicellar exchange of probe and quencher are considered was recently used, within the framework of the global analysis with the reference convolution method, to investigate molecular transport of probe and quencher in reverse micelles. Simultaneous analysis of the fluorescence decay surface obtained from the quenching of sodium 1-pyrene sulfonate by *N*-tetradecylpyridinium chloride in the reverse micellar system of *N*-benzyl-*N*,*N*-dimethyltetradecylammonium chloride in toluene indicated that the probe is a mobile species while the quencher is immobile.[134b] The absence of quencher but the presence of probe exchange was ascribed to micellar collision, inducing selective exchange. During interaction between two micelles, the probe held in the inner region of the surfactant layer of the reverse micelle is perturbed by the electrical potential induced by the presence of the counterpart micelle. Such an effect may lead to easier exchange of the probe (a counterion) than of the quencher (co-ion). Global analysis has also been used in the study of the quenching process in rodlike micelles.[168b,170] Different analytical approximations to the simulated fluorescence decay in finite or semi-infinite cylindrical micelles were evaluated for a range of aggregation numbers, diffusion coefficients, and quencher concentrations. Single-curve analysis as well as global analysis of synthetic data was used to search model appropriateness and model discrimination.[168b] In several situations, single-curve analysis failed to discriminate between competitive models. On the other hand, global analysis of decay surfaces made the discrimination possible in some situations. For instance, simultaneous analysis of fluorescence decays obtained for different quencher concentrations allowed discrimination between diffusion transients in cylindrical micelles and the process in the presence of mobile quenchers. Analysis of real experiments of the quenching process in cylindrical micelles has also proved the superior quality which can be obtained in parameter recovery with the use of simultaneous analysis.[169,170]

III.3. Lifetime Distribution Analysis of the Micelle Quenching Kinetics[193,194]

The δ-response function of several models of fluorescence quenching in micelles can be represented by a series of exponentials. For example, eq 20 can be rewritten as

$$f(t) = A_1 \exp[-A_3] \sum_{i=0} \frac{A_3^i}{i!} \exp[-(A_2 + iA_4)t] \quad (76)$$

which implies that the fluorescence decay function is a discrete set of exponentials with Poisson-distributed amplitudes and decay times located at $(A_2 + jA_4)^{-1}$. The kinetic parameters of the quenching process in micelles could then be obtained if the distribution of decay times is recovered with high precision.

Distribution analysis fluorescence quenching in micelles was introduced by Siemiarczuk and Ware.[193] They applied the maximum entropy method (MEM) for mapping the decay times patterns of the quenching process. In the MEM method, the probe function is represented by the sum

$$f(t) = \sum_{i=1}^{N} a_i \exp[-t/\tau_i] \quad (77)$$

with fixed, logarithmically spaced decay times τ_i. The amplitudes a_i are reconstructed by maximizing the entropy-like function

$$S = \sum_{i=1}^{N} a_i \ln (a_i/a_t) \quad (78)$$

where

$$a_t = \sum_{i=1}^{N} a_i \quad (79)$$

with the imposed constraint $\chi^2 \cong 1$.

The fluorescence quenching of pyrene by Cu^{2+} in SDS micelles was investigated by this method.[193a] The results indicated that the distribution of decay times is composed of a long-lived spike well separated from a short-lived, broad distribution. In the assumption of immobile probe and also considering the quenching rate constant much larger than the quencher exchange rate constant, $k_q \gg k_- + k_e[M]$, the spike is then ascribed as A_2^{-1} while the distribution to the remaining decay times $\tau_j = (A_2 + jk_q)^{-1}$, where $j = 1, 2, 3, ...$, and $A_2 = k_0 + \bar{n}k_-$. The decay rate averages over these two distinct region of the spectral patterns, $\langle 1/\tau_0 \rangle$ and $\langle 1/\tau \rangle$, and the integrated amplitude ratio, r, between the components at $j > 1$ and the spike at τ_0, are all measurable parameters, directly obtained from the MEM analysis. They are defined as

$$\langle 1/\tau_0 \rangle = \sum_m a_m \tau_m^{-1} \quad (80)$$

$$\langle 1/\tau \rangle = \sum_l a_l \tau_l^{-1} \quad (81)$$

$$r = \sum_l a_l / \sum_m a_m \quad (82)$$

where the summation indices l and m are spanning the distribution range and the τ_0 range, respectively. It has been demonstrated that those parameters are related to the model parameter in the case of Poisson distributed quenchers by

$$k_q = (\langle 1/\tau \rangle - \langle 1/\tau_0 \rangle)(1 - \exp[-\bar{n}])/\bar{n} \quad (83)$$

$$\bar{n} = \ln (r + 1) \quad (84)$$

By combining eqs 83 and 84, one can thus determine both $\bar{n}$ and k_q. The accuracy of the method was investigated on the basis of synthetic decay data. The results indicated that both $\bar{n}$ and k_q can be recovered with high precision. When applied to real decay from the quenching of pyrene by Cu^{2+} in SDS micelles, the values of k_q observed were independent of the quencher concentration and a average value $k_q = 2.26 \times 10^7$ s^{-1} was obtained which is in a good agreement with previous results obtained by direct fitting with eq 20. Also the value of the spike corresponding to A_2^{-1} was a function of the Cu^{2+} concentration as expected since this quencher is a mobile species. Contrary to the linear relationship of A_2 to the quencher concentration reported in literature,[59] an upward curvature was observed. It should be pointed out that a high occupancy can further complicate this sytem as Scaiano has shown that, in SDS at an occupancy of three of the quencher Cu^{2+}, the emission spectrum of pyrene showed a time dependence.[195]

A modified version of the method was also tested in order to investigate the possibility of direct recovery of the quencher distribution. In such a case, the decay times are positioned at $\tau_j = (A_2 + jk_q)^{-1}$ and the number of components reduced to $j \leq 15$. A_2 is taken from the previous results or from the analysis of the tail of the decay. The value of k_q is varied until the best fit is found judged by χ^2 and residuals. The recovery amplitudes can be analyzed to see if they follow a Poisson distribution. In the case of pyrene/Cu^{2+}/SDS system, the Poisson distribution of amplitudes was recovered explicitly from the fluorescence decay data. However, distribution analysis should face serious problems if the quencher exchange rate constant is of the same order as the quenching rate constants. In such a situation, these two different components may overlap difficulting the application of the method. Also the method may have the same problem if probe migration is present. In this particular case, the amplitudes of the discrete set of exponentials are no longer Poisson distributed.

IV. Conclusions

Time-resolved fluorescence quenching provides a unique method to investigate both size and molecular transport in microheterogeneous systems. The theoretical advances in fluorescence quenching in micellar assemblies obtained in the past few years have enlarged the scope of this probing method. In particular the stochastic description of the quenching process has led to a more detailed analysis of probe and quencher migration.

Time-resolved fluorescence quenching in micelles can be properly measured by a single-photon timing technique. Today it is recognized that global analysis offers advantages over single-curve analysis. The possibility of discriminating between competing models and the more accurate model parameter recovery are some of its tangible advantages. The investigation of micelle polydispersity effects on the quenching process by using polymer-forming micelles with a well-defined micellar size distribution and the molecular transport of reactants in micelle clusters and polymerized reverse micelles are topics of the future. If a select probe–quencher pair which has a decay with Poisson-distributed rate constants is chosen, then the use of a sample with known size distribution may be used to test the models of fluorescence quenching in polydisperse systems.

Acknowledgments. The authors are indebted to Dr. M. Van der Auweraer, Dr. N. Boens, and the numerous collaborators who over the years have contributed substantially to the development of the micellar research within the laboratory. In particular the availability of the global analysis program, developed by Dr. Boens was essential. M.H.G. is indebted to the KULeuven and the Brazilian Government for a scholarship. The continuing support by the Ministry of Scientific Programming through IUAP-16 and IUAP-040 is gratefully acknowledged.

Glossary

AOT	sodium bis(2-ethylhexyl) sulfosuccinate
C_0	quencher concentration in a cylindrical micelle
cmc	critical micellar concentration
CTAC	hexadecyltrimethylammonium chloride
CTAB	hexadecyltrimethylammonium bromide
D	diffusion coefficient
D_s	sum of the tangential diffusion coefficient of probe and quencher
D_c	mutual diffusion coefficient of probe and quencher in a cylindrical micelle
$\bar{d}$	fractal dimension
$\tilde{d}$	spectral dimension or fracton
DHP	dihexadecyl phosphate
$d_s(t)$	time-resolved fluorescence profile
DTAC	dodecyltrimethylammonium chloride
erfc (x)	complement of the error function
$f_s(t)$, $f'_s(t)$	sample response function and its time derivative
$\tilde{f}_s(t)$	modified sample response function
$h(r)$	distance distribution function for the donor–acceptor pair
I	fluorescence intensity observed with continuous excitation
I_0	fluorescence intensity observed with continuous excitation in the absence of added quencher
irf (t)	instrument response function
k	first-order probe migration rate constant
K	k_+/k_- = association equilibrium constant of the quencher to the micellar phase
k_e	quencher exchange rate constant
k_{exq}	generalized quencher exchange rate constant
k_f	radiative fluorescence decay rate constant
k_0	probe's excited-state decay rate constant in the absence of quencher
k_p	second-order probe migration rate constant
k_q	first-order intramicellar quenching rate constant
k_t	fusion–fission rate constant
k_+	entrance rate constant for a quencher into a micelle
k_-	exit rate constant for a quencher from a micelle
L	length of a cylindrical micelle
M_n	a micelle with n quenchers
M^*_n	a micelle with n quenchers and one excited probe
[M]	concentration of micelles
[M_n]	concentration of micelles with n quenchers
[M^*_n]	concentration of micelles with n quenchers and one excited probe
MEM	maximum entropy method

$\bar{n}$	average number of quencher per micelle
N_{agg}	average aggregation number
N_w	weight-average aggregation number
$p(r,t)$	pair distribution density
$\langle p(t) \rangle$	spatially averaged pair distribution density
$P^*_n(t)$	probability of finding a micelle with one excited probe and n quenchers
PSA	pyrenesulfonic acid, sodium salt
PTSA	pyrenetetrasulfonic acid, sodium salt
q	ratio of quencher to surfactant molecules in a micelle
$[Q]_a$	quencher concentration in the aqueous phase
$[Q]_m$	quencher concentration in the micellar phase
[Q]	total quencher concentration
R_c	radius of a cylindrical micelle
R_m	micellar radius
R_0	Förster critical radius
R_q	quencher molecular radius
R_p	probe molecular radius
R_{pq}	sum of the probe and quencher molecular radius
[S]	total surfactant concentration
SDS	sodium dodecylsulfate
TTAC	tetradecyltrimethylammonium chloride
$\langle x \rangle$, $\langle x \rangle_s$	average number of quencher in the subset of micelles with one excited probe, and its stationary value
$\delta(t)$	Dirac delta function
σ, ξ	second and third cumulants of the micellar size distribution
τ_0	donor decay time in the absence of acceptors
τ_r	decay time of the reference compound
λ_{ex}	excitation wavelength
λ_{em}	emission wavelength
χ^2	chi square

References

(1) Förster, Th.; Selinger, B. K. *Z. Naturforsch A* **1964**, *19*, 38.
(2) (a) Kalyanasundaram, K. *Chem. Soc. Rev.* **1978**, *7*, 453. (b) Kalyanasundaran, K. *Photochemistry in Microheterogeneous Systems*; Academic Press: New York, 1987.
(3) (a) Thomas J. K. *Chem. Rev.* **1980**, *80*, 283. (b) Thomas, J. K. *J. Phys. Chem.* **1987**, *91*, 267.
(4) (a) Fendler, J. H. *Chem. Rev.* **1987**, *87*, 877. (b) Fendler, J. H. *J. Phys. Chem.* **1980**, *84*, 1485.
(5) Grieser, F.; Drummond, C. J. *J. Phys. Chem.* **1988**, *92*, 5580.
(6) De Schryver, F. C.; Croonen, Y.; Geladé, E.; Van der Auweraer, M.; Dederen, J. C.; Roelants, E.; Boens, N. In *Surfactants in solution*; Mittal, K. L., Lindman, B., Eds.; Plenum Press: New York, 1984; Vol. 1, p 663.
(7) (a) Van der Auweraer, M.; Roelants, E.; Verbeeck, A.; De Schryver, F. C. In *Surfactants in Solution*; Mittal, K. L., Ed.; Plenum Press: New York, 1989; Vol. 7, p 141. (b) Van der Auweraer, M.; De Schryver, F. C. In *Structure and reactivity in reverse micelles*; Pileni, M. P., Ed.; Elsevier: Amsterdam, 1989; p 70.
(8) Tachiya, M. In *Kinetics of nonhomogeneous processes*; Freeman, G. R., Ed.; Wiley: New York, 1987; p 575.
(9) Zana, R. In *Surfactant Solutions: New Methods of Investigation*; Zana, R., Ed.; Marcel Dekker: New York, 1987; p 241.
(10) Almgren, M. In *Kinetics and catalysis in microheterogeneous systems*; Grätzel, M., Kalyanasundaram, K., Eds.; Marcel Dekker: New York, 1991; p 63.
(11) Grätzel, M. *Heterogeneous Photochemical Electron Transfer*; CRC Press: Boca Raton, FL, 1989.
(12) Tanford, C. *The Hydrophobic Effect, Formation of Micelles and Membranes*, 2nd ed.; Wiley: New York, 1980.
(13) (a) Hartley, G. S. *Aqueous solution of paraffin chain salts*; Hermann: Paris, 1936. (b) Tanford, C. *J. Phys. Chem.* **1974**, *78*, 2469. (c) Wennerström, H.; Lindman, B. *J. Phys. Chem.* **1979**, *83*, 2931.
(14) (a) Israelachvili, I. N.; Mitchell, D. J.; Nisham, B. W. *Chem. Soc., Faraday Trans. 2* **1976**, *7*, 1525. (b) Mitchel, D. J.; Ninham, B. W. *J. Chem. Soc., Faraday Trans. 2* **1981**, *77*, 601. (c) Gruen, D. W. R. *Prog. Colloid Polym. Sci.* **1985**, *70*, 6.
(15) (a) Menger, F. M. *Acc. Chem. Res.* **1979**, *12*, 111. (b) Menger, F. M.; Boyer, B. J. *J. Am. Chem. Soc.* **1980**, *102*, 5936. (c) Menger, F. M.; Boyer, B. J. *J. Am. Chem. Soc.* **1986**, *108*, 1297.
(16) Dill, K. A.; Flory, P. J. *Proc. Natl. Acad. Sci. U.S.A.* **1981**, *78*, 676.
(17) Fromherz, P. *Ber. Bunsen-Ges Phys. Chem.* **1981**, *85*, 891.
(18) (a) Aniansson, E. A. G.; Wall, S. N. *J. Phys. Chem.* **1974**, *78*, 1024. (b) Aniansson, E. A. G.; Wall, S. N. *J. Phys. Chem.* **1975**, *79*, 857. (c) Aniansson, E. A. G. *Prog. Colloid Polym. Sci.* **1985**, *70*, 2.
(19) Aniansson, E. A. G.; Wall, S. N.; Almgren, M.; Hoffman, H.; Kielmann, I.; Ulbrich, W.; Zana, R.; Lang, J.; Tondre, C. *J. Phys. Chem.* **1976**, *80*, 905.
(20) (a) Hall, D. G. *J. Chem. Soc., Faraday Trans. 2* **1981**, *77*, 1973. (b) Hall, D. G. *Colloids Surf.* **1982**, *4*, 367.
(21) Kahlweit, M.; Teubner, M. *Adv. Colloid Interface Sci.* **1980**, *13*, 1.
(22) Lessner, E.; Teubner, M.; Kahlweit, M. *J. Phys. Chem.* **1981**, *85*, 1529.
(23) (a) Kahlweit, M. *J. Colloid Interface Sci.* **1982**, *90*, 92; (b) *Pure Appl. Chem.* **1981**, *53*, 2069.
(24) Gettins, J.; Gould, C.; Hall, D. G.; Jobling, P.; Rassing, J.; Wyn-Jones, E. *J. Chem. Soc., Faraday Trans. 2* **1980**, *76*, 1535.
(25) Bloor, D.; Wyn-Jones, E. *J. Chem. Soc., Faraday Trans. 2* **1982**, *78*, 657.
(26) Johner, A.; Joanny, J. F. *Macromolecules* **1990**, *23*, 5299.
(27) Cao, T.; Munk, P.; Ramireddy, C.; Tuzar, Z.; Webber, S. E. *Macromolecules* **1991**, *24*, 6300.
(28) Gösele, U.; Klein, U. K. A.; Hauser, M. *Chem. Phys. Lett.* **1979**, *68*, 291.
(29) Tachiya, M. *Chem. Phys. Lett.* **1980**, *69*, 605.
(30) Hatlee, M. D.; Kozak, J. J.; Rothenberger, G.; Infelta, P. P.; Grätzel, M. *J. Phys. Chem.* **1980**, *84*, 1508.
(31) Van der Auweraer, M.; Dederen, J. C.; Geladé, E.; De Schryver, F. C. *J. Chem. Phys.* **1981**, *74*, 1140.
(32) Sano, H.; Tachiya, M. *J. Chem. Phys.* **1981**, *75*, 2870.
(33) Hatlee, M. D.; Kozak, J. J.; Grätzel, M. *Ber. Bunsen-Ges Phys. Chem.* **1982**, *86*, 157.
(34) (a) Rothenberger, G.; Grätzel, M. *Chem. Phys. Lett.* **1989**, *154*, 165. (b) Rothenberger, G.; Infelta, P. P. In *Kinetics and catalysis in microheterogeneous systems, surfactant science series*, Grätzel, M., Kalyanasundaran, K., Eds.; Marcel Dekker: New York, 1991; Vol. 38, p 49.
(35) Marqusee, J. A.; Dill, K. A. *J. Chem. Phys.* **1986**, *85*, 434.
(36) Kalyanasundaram, K. In *Photochemistry in Organized and Constrained Media*; Ramamurthy, V., Ed.; VCH Publishers: New York, 1991; p 39.
(37) Steinberg, Z.; Katchalski, E. *J. Chem. Phys.* **1968**, *48*, 2404.
(38) Infelta, P. P.; Grätzel, M.; Thomas, J. K. *J. Phys. Chem.* **1974**, *78*, 190.
(39) Tachiya, M. *Chem. Phys. Lett.* **1975**, *33*, 289.
(40) Maestri, M.; Infelta, P. P.; Grätzel, M. *J. Chem. Phys.* **1978**, *69*, 1522.
(41) Rodgers, M. A. J.; Da Silva e Wheeler, M. F. *Chem. Phys. Lett.* **1978**, *53*, 165.
(42) Infelta, P. P.; Grätzel, M. *J. Chem. Phys.* **1979**, *70*, 179.
(43) Dederen, J. C.; Van der Auweraer, M.; De Schryver, F. C. *Chem. Phys. Lett.* **1979**, *68*, 451.
(44) Hatlee, M. D.; Kozak, J. J. *J. Chem. Phys.* **1980**, *72*, 4358.
(45) (a) Rothenberger, G.; Infelta, P. P.; Grätzel, M. *J. Phys. Chem.* **1979**, *83*, 1871. (b) Rothenberger, G.; Infelta, P. P.; Grätzel, M. *J. Phys. Chem.* **1981**, *85*, 1850.
(46) Vass, Sz. *Chem. Phys. Lett.* **1980**, *70*, 135.
(47) Tachiya, M. *J. Chem. Phys.* **1982**, *76*, 340.
(48) Webber, S. E. *J. Phys. Chem.* **1983**, *87*, 347.
(49) (a) Almgren, M.; Löfroth, J. E.; van Stam, J. *J. Phys. Chem.* **1986**, *90*, 4431. (b) Almgren, M.; Stam, J. van; Swarup, S.; Löfroth, J. E. *Langmuir* **1986**, *2*, 432.
(50) Tachiya, M. *Can. J. Phys.* **1990**, *68*, 979.
(51) Gehlen, M. H.; Van der Auweraer, M.; Reekmans, S.; Neumann, M.; De Schryver, F. C. *J. Phys. Chem.* **1991**, *95*, 5684.
(52) Gehlen, M. H.; Van der Auweraer, M.; De Schryver, F. C. *Photochem. Photobiol.* **1991**, *54*, 613.
(53) Barzykin, A. V.; Razumov, V. F.; Alfimov, M. V. *J. Phys. Chem.* **1991**, *95*, 4814.
(54) Barzykin, A. V. *Chem. Phys. Lett.* **1992**, *189*, 321.
(55) Yekta, A.; Aikawa, M.; Turro, N. *J. Chem. Phys. Lett.* **1979**, *63*, 543.
(56) Infelta, P. P.; Grätzel, M. *Chem. Phys. Lett.* **1979**, *61*, 88.
(57) Atik, S. S.; Nam, M.; Singer, L. A. *Chem. Phys. Lett.* **1979**, *67*, 75.
(58) Atik, S. S.; Singer, L. A. *Chem. Phys. Lett.* **1979**, *66*, 234.
(59) Dederen, J. C.; Van der Auweraer, M.; De Schryver, F. C. *J. Phys. Chem.* **1981**, *85*, 1198.
(60) Ziemiecki, H.; Cherry, W. R. *J. Am. Chem. Soc.* **1981**, *103*, 4479.
(61) Grieser, F.; Tausch-Treml, R. *J. Am. Chem. Soc.* **1980**, *102*, 7258.
(62) Grieser, F. *Chem. Phys. Lett.* **1981**, *83*, 59.
(63) Waka, F.; Hamamoto, K.; Mataga, N. *Photochem. Photobiol.* **1980**, *32*, 27.
(64) Pileni, M. P.; Grätzel, M. *J. Phys. Chem.* **1980**, *84*, 1822.
(65) Almgren, M.; Löfroth, J. E. *J. Colloid Interface Sci.* **1980**, *81*, 486.
(66) Rodgers, M. A. J.; Baxandale, J. H. *Chem. Phys. Lett.* **1981**, *81*, 347.
(67) Atherton, S. J.; Baxandale, J. H.; Hoey, B. M. *J. Chem. Soc., Faraday Trans. 1* **1982**, *78*, 2167.
(68) Löfroth, J. E.; Almgren, M. *J. Phys. Chem.* **1982**, *86*, 1636.
(69) Van der Auweraer, M.; Dederen, J. C.; Palmans-Windels, C.; De Schryver, F. C. *J. Am. Chem. Soc.* **1982**, *104*, 1800.

(70) Lianos, P.; Lang, J.; Strazielle, C.; Zana, R. *J. Phys. Chem.* **1982**, *86*, 1019.
(71) Lianos, P.; Lang, J.; Zana, R. *J. Phys. Chem.* **1982**, *86*, 4809.
(72) Lianos, P.; Lang, J.; Sturm, J.; Zana, R. *J. Phys. Chem.* **1984**, *88*, 819.
(73) Levitz, P.; Van Damme, H.; Keravis, D. *J. Phys. Chem.* **1984**, *88*, 2228.
(74) (a) Miyashita, T.; Murakata, T.; Matsuda, M. *J. Phys. Chem.* **1983**, *87*, 4529. (b) Miyashita, T.; Murakata, T.; Matsuda, M. *J. Phys. Chem.* **1989**, *93*, 1426.
(75) Miyashita, T.; Murakata, T.; Yamaguchi, Y.; Matsuda, M. *J. Phys. Chem.* **1985**, *89*, 497.
(76) Croonen, Y.; Geladé, E.; Van der Zegel, M.; Van der Auweraer, M.; Vanderdriessche, H.; De Schryver, F. C.; Almgren, M. *J. Phys. Chem.* **1983**, *87*, 1426.
(77) Geladé, E.; De Schryver, F. C. *J. Am. Chem. Soc.* **1984**, *106*, 5871.
(78) Abdel-Kader, M. H.; Braun, A. M. *J. Chem. Soc., Faraday Trans. 1* **1985**, *81*, 245.
(79) Roelants, E.; Geladé, E.; Smid, J.; De Schryver, F. C. *J. Colloid Interface Sci.* **1985**, *107*, 337.
(80) Roelants, E.; De Schryver, F. C. *Langmuir* **1987**, *3*, 209.
(81) Zana, R.; Guveli, D. *J. Phys. Chem.* **1985**, *89*, 1687.
(82) Malliaris, A.; Binana-Limbele, W.; Zana, R. *J. Colloid Interface Sci.* **1986**, *110*, 114.
(83) Malliaris, A.; Lang, J.; Zana, R. *J. Chem. Soc., Faraday Trans. 1* **1986**, *82*, 109.
(84) Malliaris, A.; Lang, J.; Sturm, J.; Zana, R. *J. Phys. Chem.* **1987**, *91*, 1475.
(85) (a) Boens, N.; Malliaris, A.; Van der Auweraer, M.; Luo, H.; De Schryver, F. C. *Chem. Phys.* **1988**, *121*, 199. (b) Boens, N.; Luo, H.; Van der Auweraer, M.; Reekmans, S.; De Schryver, F. C.; Malliaris, A. *Chem. Phys. Lett.* **1988**, *146*, 337.
(86) Reekmans, S.; Boens, N.; Van der Auweraer, M.; Luo, H.; De Schryver, F. C. *Langmuir* **1989**, *5*, 948.
(87) Luo, H.; Boens, N.; Van der Auweraer, M.; De Schryver, F. C.; Malliaris, A. *J. Phys. Chem.* **1989**, *93*, 3244.
(88) Reekmans, S.; Luo, H.; Van der Auweraer, M.; De Schryver, F. C. *Langmuir* **1990**, *6*, 628.
(89) Miller, D. D.; Evans, D. F. *J. Phys. Chem.* **1989**, *93*, 323.
(90) Chen, M.; Grätzel, M.; Thomas, J. K. *J. Am. Chem. Soc.* **1975**, *97*, 2052.
(91) Kalyanasundaram, K.; Grätzel, M.; Thomas, J. K. *J. Am. Chem. Soc.* **1975**, *97*, 3915.
(92) Aikawa, M.; Yekta, A.; Turro, N. J. *Chem. Phys. Lett.* **1979**, *68*, 285.
(93) Selinger, B. K.; Watkins, A. R. *Chem. Phys. Lett.* **1978**, *56*, 99.
(94) Turro, N. J.; Yekta, A. *J. Am. Chem. Soc.* **1978**, *100*, 5951.
(95) (a) Almgren, M.; Swarup, S. *J. Phys. Chem.* **1982**, *86*, 4212. (b) Almgren, M.; Swarup, S. *J. Colloid Interface Sci.* **1983**, *91*, 256.
(96) Brady, J. E.; Evans, D. F.; Warr, G. G.; Grieser, F.; Ninham, B. W. *J. Phys. Chem.* **1986**, *90*, 1853.
(97) (a) Encinas, V.; Lissi, E. A. *Chem. Phys. Lett.* **1982**, *91*, 55. (b) Encinas, V.; Lissi, E. A. *Chem. Phys. Lett.* **1986**, *132*, 545. (c) Encinas, V.; Lissi, E. A. *Photochem. Photobiol.* **1983**, *37*, 251. (d) Encinas, V.; Guzman, E.; Lissi, E. A. *J. Phys. Chem.* **1983**, *87*, 4770.
(98) Sepulveda, L.; Lissi, E. A.; Quina, F. H. *Adv. Colloid Interface Sci.* **1986**, *25*, 1.
(99) (a) Leigh, W. J.; Scaiano, J. C. *J. Am. Chem. Soc.* **1983**, *105*, 5652. (b) Kim-Thuan, N.; Scaiano, J. C. *Chem. Phys. Lett.* **1983**, *101*, 192.
(100) (a) Blatt, E.; Chatelier, R. C.; Sawyer, W. H. *Chem. Phys. Lett.* **1984**, *108*, 397. (b) Blatt, E.; Chatelier, R. C.; Sawyer, W. H. *Biophys. J.* **1986**, *50*, 349.
(101) Gehlen, M. H.; Berci, Fo, P.; Neumann, M. G. *J. Photochem. Photobiol. A: Chem.* **1991**, *59*, 335.
(102) Henglein, A.; Proske, Th. *Ber. Bunsen-Ges Phys. Chem.* **1978**, *82*, 471.
(103) (a) Frank, A. J.; Grätzel, M.; Kozak, J. J. *J. Am. Chem. Soc.* **1976**, *98*, 3317. (b) Moroi, Y.; Braun, A. M.; Grätzel, M. *J. Am. Chem. Soc.* **1979**, *101*, 567. (c) Moroi, Y.; Infelta, P. P.; Grätzel, M. *J. Am. Chem. Soc.* **1979**, *101*, 573.
(104) Almgren, M.; Gunnarsson, G.; Linse, P. *Chem. Phys. Lett.* **1982**, *85*, 451.
(105) Almgren, M.; Linse, P.; Van der Auweraer, M.; De Schryver, F. C.; Geladé, E.; Croonen, Y. *J. Phys. Chem.* **1984**, *88*, 289.
(106) Almgren, M.; Stilbs, P.; Alsins, J.; Linse, P.; Kamenka, N. *J. Phys. Chem.* **1985**, *89*, 2666.
(107) Eicke, H. F.; Shepherd, J. C. W.; Steinemann, A. *J. Colloid Interface Sci.* **1976**, *56*, 168.
(108) (a) Roux, D.; Bellocq, A. M.; Bothorel, P. *Prog. Colloid Polym. Sci.* **1984**, *69*, 1. (b) Zemb, T. N.; Barnes, I. S.; Derian, P. J.; Ninham, B. W. *Progr. Colloid Polym. Sci.* **1990**, *81*, 20.
(109) Gregortich, S. J.; Thomas, J. K. *J. Phys. Chem.* **1980**, *84*, 1491.
(110) (a) Atik, S. S.; Thomas, J. K. *J. Phys. Chem.* **1981**, *85*, 3921. (b) Atik, S. S.; Thomas, J. K. *J. Am. Chem. Soc.* **1981**, *103*, 4367. (c) Atik, S. S.; Thomas, J. K. *Chem. Phys. Lett.* **1981**, *79*, 351.
(111) Fletcher, P. D. I.; Robinson, B. H. *Ber. Bunsen-Ges Phys. Chem.* **1981**, *85*, 863.
(112) Geladé, E.; De Schryver, F. C. *J. Photochem.* **1982**, *18*, 223.
(113) Bridge, N. J.; Fletcher, P. D. I. *J. Chem. Soc., Faraday Trans. 1* **1983**, *79*, 2161.
(114) Brochette, P.; Pileni, M. P. *Nouv. J. Chim.* **1985**, *9*, 551.
(115) Verbeeck, A.; De Schryver, F. C. *Langmuir* **1987**, *3*, 494.
(116) (a) Fletcher, P. D. I.; Howe, A. M.; Robinson, B. H. *J. Chem. Soc., Faraday Trans. 1* **1987**, *83*, 985. (b) Howe, A. M.; Mc Donald, J. A.; Robinson, B. H. *J. Chem. Soc., Faraday Trans. 1* **1987**, *83*, 1007.
(117) Kikachi, K.; Thomas, J. K. *Chem. Phys. Lett.* **1988**, *148*, 245.
(118) Lang, J.; Jada, A.; Malliaris, A. *J. Phys. Chem.* **1988**, *92*, 1946.
(119) (a) Jada, A.; Lang, J.; Zana, R. *J. Phys. Chem.* **1989**, *93*, 10. (b) Jada, A.; Lang, J.; Zana, R.; Makhloufi, R.; Hirsch, E.; Candau, S. J. *J. Phys. Chem.* **1990**, *94*, 387. (c) Lang, J.; Mascolo, G.; Zana, R.; Luisi, P. L. *J. Phys. Chem.* **1990**, *94*, 3069. (d) Lang, J.; Lalem, N.; Zana, R. *J. Phys. Chem.* **1991**, *95*, 9533.
(120) Verbeeck, A.; Voortmans, G.; Jackers, C.; De Schryver, F. C. *Langmuir* **1989**, *5*, 766.
(121) Johannsson, R.; Almgren, M.; Alsins, J. *J. Phys. Chem.* **1991**, *95*, 3818.
(122) (a) Clark, S.; Fletcher, P. D. I.; Ye, X. *Langmuir* **1990**, *6*, 1301. (b) Fletcher, P. D. I.; Horsup, D. I. *J. Chem. Soc., Faraday Trans.* **1992**, *88*, 855.
(123) (a) Chu, D. Y.; Thomas, J. K. *Macromolecules* **1984**, *17*, 2142. (b) Chu, D. Y.; Thomas, J. K. *Macromolecules* **1987**, *20*, 2133. (c) Chu, D. Y.; Thomas, J. K. *J. Phys. Chem.* **1985**, *89*, 4065. (d) Chu, D. Y.; Thomas, J. K. *J. Am. Chem. Soc.* **1986**, *108*, 6270.
(124) (a) Winnik, F. M.; Winnik, M. A.; Tazuke, S. *J. Phys. Chem.* **1987**, *91*, 594. (b) Winnik, F. M.; Winnik, M. A. *Polym. J.* **1990**, *22*, 482.
(125) Lissi, E. A.; Abuin, E. *J. Colloid Interface Sci.* **1985**, *105*, 1.
(126) Zana, R.; Lianos, P.; Lang, J. *J. Phys. Chem.* **1985**, *89*, 41.
(127) Limbele, W. B.; Zana, R. *Colloid Surf.* **1986**, *21*, 483.
(128) Hsu, J. L.; Strauss, U. P. *J. Phys. Chem.* **1987**, *91*, 6238.
(129) (a) Stam, J. van; Almgren, M.; Lindblad, C. *Progr. Colloid Polym. Sci.* **1991**, *84*, 13. (b) Almgren, M.; Alsins, J.; Bahadur, P. *Langmuir* **1991**, *7*, 446. (c) Thalberg, K.; Stam. J. van; Lindblad, C.; Almgren, M.; Lindman, B. *J. Phys. Chem.* **1991**, *95*, 8975.
(130) Caminati, G.; Tomalia, D. A.; Turro, N. J. *Progr. Colloid Polym. Sci.* **1991**, *84*, 219.
(131) Reekmans, S.; Gehlen, M. H.; De Schryver, F. C.; Van der Auweraer, M., submitted.
(132) Reekmans, S.; De Schryver, F. C. In *Frontiers in Supramolecular Organic Chemistry and Photochemistry*; Schneider, H., Durr, H., Eds.; VCH: Weinheim, 1991; p 287.
(133) Gehlen, M. H.; Van der Auweraer, M.; De Schryver, F. C. *Langmuir* **1992**, *8*, 64.
(134) (a) Gehlen, M. H.; Boens, N.; De Schryver, F. C.; Van der Auweraer, M.; Reekmans, S. *J. Phys. Chem.* **1992**, *96*, 5592. (b) Gehlen, M. H.; Boens, N.; Van der Auweraer, M.; De Schryver, F. C., submitted.
(135) Brown, W.; Rymdén, R.; Stam, J. van; Almgren, M.; Svensk, G. *J. Phys. Chem.* **1989**, *93*, 2512.
(136) Lindman, B.; Wennerström, H. *J. Phys. Chem.* **1991**, *95*, 6053.
(137) Odijk, T. *Biophys. Chem.* **1991**, *41*, 23.
(138) Kotlarchyk, M.; Stephens, R. B.; Huang, J. S. *J. Phys. Chem.* **1988**, *92*, 1533.
(139) Eriksson, J. C.; Ljunggren, S. *Prog. Colloid Polym. Sci.* **1990**, *81*, 41.
(140) (a) Almgren, M.; Lôfroth, J. E. *J. Chem. Phys.* **1982**, *76*, 2734. (b) Lôfroth, J. E.; Almgren, M. In *Surfactants in solution*; Mittal, K. L., Lindman, B., Eds.; Plenum Press: New York, 1984; p 627.
(141) Malliaris, A.; Le Moigne, J.; Sturm, J.; Zana, R. *J. Phys. Chem.* **1985**, *89*, 2709.
(142) Zana, R.; Weill, C. *Chem. Phys. Lett.* **1985**, *46*, 935.
(143) Lang, J. *J. Phys. Chem.* **1990**, *94*, 3734.
(144) (a) Warr, G. G.; Grieser, F. *J. Chem. Soc., Faraday Trans. 1* **1986**, *82*, 1829. (b) Warr, G. G.; Grieser, F.; Evans, D. F. *J. Chem. Soc., Faraday Trans. 1* **1986**, *82*, 1829.
(145) Warr, G. G.; Drummond, C. J.; Grieser, F.; Ninham, B. W.; Evans, D. F. *J. Phys. Chem.* **1986**, *90*, 4581.
(146) Miller, D. J. *J. Chem. Educ.* **1978**, *55*, 776.
(147) Hunter, T. *Chem. Phys. Lett.* **1980**, *75*, 152.
(148) Nakamura, T.; Kira, A.; Imamura, M. *J. Phys. Chem.* **1983**, *87*, 3122.
(149) Warr, G. G.; Grieser, F. *Chem. Phys. Lett.* **1985**, *116*, 505.
(150) Habti, A.; Keravis, D.; Levitz, P.; Van Damme, H. *J. Chem. Soc., Faraday Trans. 2* **1984**, *80*, 67.
(151) (a) Martens, F. M.; Verhoeven, J. W. *J. Phys. Chem.* **1981**, *85*, 1773. (b) Russel, J. C.; Whitten, D. G. *J. Am. Chem. Soc.* **1981**, *103*, 3219.
(152) Timpe, H. J.; Israel, G.; Becker, H. G. O.; Gould, I. R.; Turro, N. J. *Chem. Phys. Lett.* **1983**, *99*, 275.
(153) Blatt, E. *J. Phys. Chem.* **1986**, *90*, 874.
(154) Singhal, G. S.; Rabinowitch, E.; Hevesi, J.; Srinivasan, V. *Photochem. Photobiol.* **1970**, *11*, 531.
(155) Almgren, M. *Photochem. Photobiol.* **1972**, *15*, 297.
(156) Wallace, G. A. K.; Flint, J. H.; Wallace, S. C. *Chem. Phys. Lett.* **1975**, *32*, 71.
(157) Matsuo, T.; Aso, Y.; Kano, K. *Ber. Bunsen-Ges Phys. Chem.* **1980**, *84*, 146.
(158) Sato, H.; Kawasaki, M.; Kasatani, K. *J. Phys. Chem.* **1983**, *87*, 3759.
(159) Koglin, P. K. F.; Miller, D. J.; Steinwandel, J.; Hauser, M. *J. Phys. Chem.* **1981**, *85*, 2363.

(160) Ediger, M. D.; Domingue, R. P.; Fayer, M. D. *J. Chem. Phys.* **1984**, *80*, 1246.
(161) Kasatani, K.; Kawasaki, M.; Sato, H.; Nakashima, N. *J. Phys. Chem.* **1985**, *89*, 542.
(162) Berberan-Santos, M. N.; Prieto, M. J. E. *J. Chem. Soc., Faraday Trans. 2* **1987**, *83*, 1391.
(163) Kaschke, M.; Kittelmann, O.; Vogler, K.; Graness, A. *J. Phys. Chem.* **1988**, *92*, 5998.
(164) Choi, K. J.; Turkevich, L. A.; Loza, R. *J. Phys. Chem.* **1988**, *92*, 2238.
(165) Priyadarsini, K. I.; Mishra, B. K.; Manohar, C. *Chem. Phys. Lett.* **1991**, *182*, 608.
(166) (a) Barzykin, A. V. *Chem. Phys.* **1991**, *155*, 221. (b) Barzykin, A. *Chem. Phys.* **1992**, *161*, 63.
(167) Berberan-Santos, M. N.; Prieto, M. J. E.; Szabo, A. G. *J. Chem. Soc., Faraday Trans.* **1992**, *88*, 255.
(168) (a) Van der Auweraer, M.; De Schryver, F. C. *Chem. Phys.* **1987**, *111*, 105. (b) Van der Auweraer, M.; Reekmans, S.; Boens, N.; De Schryver, F. C. *Chem. Phys.* **1989**, *132*, 91.
(169) (a) Almgren, M.; Alsins, J.; Mukhtar, E.; van Stam, J. *J. Phys. Chem.* **1988**, *92*, 4479. (b) Almgren, M.; Alsins, J.; Mukhtar, E.; van Stam, J. *Prog. Colloid Polym. Sci.* **1988**, *76*, 68.
(170) (a) Alsins, J.; Almgren, M. *J. Phys. Chem.* **1990**, *94*, 3062. (b) Alsins, J.; Almgren, M. *Progr. Colloid Polym. Sci.* **1990**, *81*, 9.
(171) Klafter, J.; Drake, J. M.; Blumen, A. In *Kinetics and Catalysis in Microheterogeneous Systems*; Kalyanasundaram, K., Grätzel, M., Eds.; Marcel Dekker: New York, 1991; p 491, and references therein.
(172) Tamai, N.; Yamazaki, T.; Yamazaki, I.; Mataga, N. Ultrafast Phenomena. *Springer Ser. Chem. Phys.* **1986**, *46*, 449.
(173) Takami, A.; Mataga, N. *J. Phys. Chem.* **1987**, *91*, 618.
(174) Argyrakis, P.; Duportail, G.; Lianos, P. *J. Chem. Phys.* **1991**, *95*, 3808.
(175) Davenport, L.; Knutson, J. R.; Brand, L. *Faraday Discuss. Chem. Soc.* **1986**, *81*, 81.
(176) (a) Lianos, P.; Modes, S. *J. Phys. Chem.* **1987**, *91*, 6088. (b) Lianos, P. *J. Chem. Phys.* **1988**, *89*, 5237. (c) Modes, S.; Lianos, P. *J. Phys. Chem.* **1989**, *93*, 5854. (d) Lianos, P.; Duportail, G. *Prog. Colloid Polym. Sci.* **1991**, *84*, 151. (e) Velazquez, M. M.; Costa, S. M. B. *Chem. Phys. Lett.* **1992**, *190*, 247.
(177) Gauduchon, P.; Wahl, P. *Biophys. Chem.* **1978**, *8*, 78.
(178) Wijnaendts van Resandt, R. W.; Vogel, R. H.; Provencher, S. W. *Rev. Sci. Instrum.* **1982**, *53*, 1392.
(179) Zuker, M.; Szabo, A. G.; Bramall, L.; Krajcarshi, D. T.; Selinger, B. *Rev. Sci. Instrum.* **1985**, *56*, 14.
(180) Löfroth, J. E. *Eur. Biophys. J.* **1985**, *13*, 45.
(181) (a) Boens, N.; Van den Zegel, M.; De Schryver, F. C. *Chem. Phys. Lett.* **1984**, *111*, 340. (b) Van den Zegel, M.; Boens, N.; Daems, D.; De Schryver, F. C. *Chem. Phys.* **1986**, *101*, 311. (c) Boens, N.; Ameloot, M.; Yamazaki, I.; De Schryver, F. C. *Chem. Phys.* **1988**, *121*, 73. (d) Boens, N. In *Luminescence techniques in chemical and biochemical analysis*; Baeyens, W. R. G., Keukeleire, D., Korkidis, K., Eds.; Marcel Dekker: New York, 1991; p 21, and references therein.
(182) Ameloot, M.; Beechem, J. M.; Brand, L. *Biophys. Chem.* **1986**, *23*, 155.
(183) O'Connor, D. V.; Phillips, D. *Time-correlated single photon counting*; Academic Press: New York, 1984.
(184) Marquart, D. W. *J. Soc. Ind. Appl. Math.* **1963**, *11*, 431.
(185) Grinvald, A.; Steinberg, I. Z. *Anal. Biochem.* **1974**, *59*, 583.
(186) (a) Durbin, J.; Watson, G. S. *Biometrika* **1950**, *37*, 409. (b) Durbin, J.; Watson, G. S. *Biometrika* **1951**, *38*, 159. (c) Durbin, J.; Watson, G. S. *Biometrika* **1971**, *58*, 1.
(187) Draper, N. R.; Smith, H. *Applied regression analysis*, 2nd ed.; Wiley: New York, 1981.
(188) (a) Knutson, J. R.; Beechem, J. M.; Brand, L. *Chem. Phys. Lett.* **1983**, *102*, 501. (b) Beechem, J. M.; Knutson, J. R.; Brand, L. *Photochem. Photobiol.* **1983**, *37*, 520. (c) Beechem, J. M.; Ameloot, M.; Brand, L. *Anal. Instrum.* **1985**, *14*, 379.
(189) (a) Boens, N.; Janssens, L. D.; De Schryver, F. C. *Biophys. Chem.* **1989**, *33*, 77. (b) Janssens, L. D.; Boens, N.; Ameloot, M.; De Schryver, F. C. *J. Phys. Chem.* **1990**, *94*, 3564.
(190) (a) Löfroth, J. E. *Anal. Instrum.* **1985**, *14*, 403. (b) Löfroth, J. E. *J. Phys. Chem.* **1986**, *90*, 1160.
(191) (a) Beechem, J. M.; Ameloot, M.; Brand, L. *Chem. Phys. Lett.* **1985**, *120*, 466. (b) Ameloot, M.; Beechem, J. M.; Brand, L. *Chem. Phys. Lett.* **1986**, *129*, 211.
(192) (a) Ameloot, M.; Boens, N.; Andriessen, R.; Van der Bergh, V.; De Schryver, F. C. *J. Phys. Chem.* **1991**, *95*, 2041. (b) Andriessen, R.; Boens, N.; Ameloot, M.; De Schryver, F. C. *J. Phys. Chem.* **1991**, *95*, 2047.
(193) (a) Siemiarczak, A.; Ware, W. R. *Chem. Phys. Lett.* **1989**, *160*, 285. (b) Ware, W. R. In *Photochemistry in organized and constrained media*; Ramamurthy, V., Ed.; VCH Publishers: New York, 1991; p 563.
(194) (a) Siemiarczak, A.; Ware, W. R. *Chem. Phys. Lett.* **1990**, *167*, 263. (b) Siemiarczak, A.; Wagner, B. D.; Ware, W. R. *J. Phys. Chem.* **1990**, *94*, 1661.
(195) Jay, J.; Johnston, L. J.; Scaiano, J. C. *Chem. Phys. Lett.* **1988**, *148*, 517.